PHOTOVOLTAGE AT A METAL TO DIAMOND CONTACT

By

CLYDE JOHN MARSHALL NORTHRUP, JR.

Bachelor of Science
Oklahoma State University
Stillwater, Oklahoma
1961

Submitted to the Faculty of the Graduate School of
the Oklahoma State University
in partial fulfillment of the requirements
for the degree of
DOCTOR OF PHILOSOPHY
May, 1966

PHOTOVOLTAGE AT A METAL TO

DIAMOND CONTACT

William J. Leivo
Thesis Adviser

Harry D Crawford

Leon W. Schroeder

Louis P. Varga

J. H. Mendenhall

J. H. Boggs
Dean of the Graduate School

ACKNOWLEDGEMENTS

The assistance of many people aided in the success of this investigation. In particular, I want to express my deep gratitude to Dr. W. J. Leivo for the opportunity to do this research and for his valuable council. Drs. H. D. Crawford, H. S. Mendenhall, L. W. Schroeder, L. P. Varga, and H. E. Harrington gave me guidance throughout this study, and I thank them.

I am indebted to Professor F. C. Harris, and Drs. M. D. Bell, K. J. Russell, J. B. Krumme and W. F. Wei for their enlightning discussions. I am particularly grateful to J. P. King for his generous assistance and helpful comments. Dr. J. H. Venable and his family generously shared their home with me in the final weeks of this study, and I thank them.

The members of the Physics-Chemistry shop and the Chemistry glass shop were very helpful in the design and construction of several pieces of equipment, and I wish to thank them.

For making the semiconducting diamonds available to the group at Oklahoma State University I thank Dr. J. F. H. Custers of Industrial Distributors (1946) Limited, Dr. H. B. Dyer of the Diamond Research Laboratory, and Dr. Switzer of the U. S. National Museum.

I am grateful for the financial support of this research by

the Electronic Systems Division, Air Force Systems Command, Laurence G. Hanscom Field, Bedford, Massachusetts and the National Science Foundation, Washington, District of Columbia.

Above all, I thank my wife, Lu.

TABLE OF CONTENTS

LIST OF TABLES

LIST OF FIGURES

Figure Page

CHAPTER I

INTRODUCTION

Preliminary Remarks

It has been recognized for many years that a voltage would sometimes be produced at a diamond to metal contact when it was exposed to light. Early measurements of the photovoltage were greatly hampered since its behavior was difficult to predict and the voltage was low in magnitude. This study was undertaken to gain a more detailed knowledge of the nature of the photovoltage at a diamond to metal contact and to obtain information on the energy band structure at the diamond surface. The photovoltage was investigated as to spectral response, light intensity, temperature dependence, diamond bulk and surface properties, types of metals and methods of contacts. The related phenomena of photoconductivity and optical absorption were examined at temperatures down to 77°K in order to correlate them with the photovoltage.

The present chapter gives a brief description of diamonds and a survey of previous diamond research. The previous work on photovoltage in diamond is described in this chapter. Chapter II includes a theoretical treatment of the photovoltage as it applies to diamonds. The basic definitions and processes associated with the photovoltage are given here. Chapter III contains a description of the diamonds examined in this study and outlines the procedures and results of the measure-

ments. In Chapter IV the results are correlated and discussed.

Physical Properties of Diamond

The diamond crystal is composed of carbon atoms situated so as to form the vertices of a regular tetrahedron about a central carbon atom. Each carbon atom is then surrounded by four other carbon atoms. The diamond structure can be represented by two interpenetrating face centered cubic lattices. The interpenetrating lattices have corresponding lattice vectors which are parallel, and one lattice is displaced one-fourth of the way along a unit cell diagonal with respect to the other. Each carbon atom is bound to its four nearest neighbors by covalent bonds, and all valence electrons are shared in pairs.

Previous Research on Diamond

The interest in diamond is indicated by the volume of the previous research on this material. A continuously increasing list of publications on diamond has been compiled by our research group. Over one thousand publications pertaining to diamond have now been recorded by this group. Since a complete survey of the literature on diamond would be voluminous, only the work of special interest to the present investigation will be reviewed here.

In 1934, Robertson, Fox, and Martin (1) published a comprehensive study of diamond, and among the phenomena they observed was the photovoltage in diamond. They also examined the optical absorption and photoconductivity in diamond. On the basis of the optical absorption, they classified diamonds into two types. Type I diamond which is found

more abundantly, exhibits infrared absorption at 8μ and has an ultraviolet cutoff at wavelengths longer than 3000 A. Type II diamond does not absorb at 8μ and transmits the ultraviolet wavelengths down to 2300 A. In general, Type II diamonds showed stronger photoconductivity and photovoltages. Robertson, Fox, and Martin encountered difficulties in interpreting the photovoltage. Only on three points of one diamond were they able to consistently repeat polarities of an illuminated contact. This diamond had internal barriers, and they suggested the photovoltage might be associated with these barriers. A slight movement of the contact was apt to change the magnitude of the photovoltage and possibly even make the polarity change sign. Robertson, Fox, and Martin also noted that the diamond showing the strongest photovoltage also displayed the strongest flourescence and phosphorescence. However, not many of the diamonds examined by them showed a strong flourescence or phosphorescence; therefore, no correlation was attempted between color and strength of flourescence, and diamond type. Robertson, Fox, and Martin examined the temperature dependence of the photovoltage at lower temperatures, and comments on their results will be made in Chapter IV.

The research in diamond received a new stimulus when Custers (2,3) found that a particularly rare diamond specimen was an electrical conductor. He examined twenty-one diamonds with this new property. All were blue in color and showed a blue phosphorescence. The spectrum of the phosphorescence showed a broad continuous band with the relative maximum strongest at 4665 A. Other maxima occurred at 5310 and 5720 A. These rare diamonds were optically similar to Type II diamonds so he

classified the diamonds with these new properties as Type IIb.

Leivo and Smoluchowski (4) found that Type IIb diamonds behave like an impurity activated semiconductor. They found that the slope at room temperature of k log ρ versus 1/T equals 0.35 ev. Subsequently Brophy (5) derived an activation energy of 0.35 ev from measurements of the resistivity and Hall coefficient.

The photovoltaic effect in Type IIb diamond was studied at room temperature by Bell and Leivo (6). They found photovoltage maxima at 0.44μ, 0.66μ, and 0.89μ. As in earlier studies, they were confronted with the problems of low voltages and unpredictable polarities. They could, however, correlate the last two peaks with the photoconductivity peaks in this region, but the peak at 0.44μ was more difficult to interpret. This will be discussed further in Chapter III.

Many investigators have examined the optical absorption of diamond. The results of recent extensive studies by Charrette (7,8) are tabulated in Table 1.

All diamonds have some broad absorption bands in common. These absorption peaks occur near 2.64, 2.77, 3.16, 4.03, 4.6, and 5.0μ according to Robertson, Fox, and Martin (1). Collins and Fan (9), on the basis of the temperature dependence of these bands, suggested that these bands were characterictic of the lattice. By assuming the dipole moment of a lattice mode to be proportional to the root-mean-square thermal displacement, and the absorption to be proportional to the mean square thermal displacement, they related the change in absorption with temperature by a theoretical curve of Lonsdale's.(10). Lonsdale had shown that in diamond the mean square thermal displacement of atoms varied slowly as a function of temperature. This was a consequence of

TABLE I

INFRARED ABSORPTION IN DIAMOND (MICRONS)

I. Bands Common to all Diamonds:

A. Group at 5 microns: 5.06, 4.98, 4.92, 4.89, 4.83, 4.75, 4.67, 4.63, 4.57

B. Group at 4 microns: 4.10, 4.02, 3.94

C. Group at 3 microns: 3.25, 2.90

II. Bands Common to Type I Diamonds:

A. Group at 8 microns: 9.18, 8.48, 8.2, 7.8, 7.64

B. Very narrow bands: 7.12, 3.59, 3.22, 3.17, 3.07, 2.22

C. Narrow bands: 7.52, 7.33

D. Broad Bands: 13.5, 13.0, 10.8, 10.0, 6.6, 6.5

III. Bands Common to Type IIb Diamonds:

A. Group at 7.70 not resolved

B. Group at 4.07

C. Group at 3.56 with complex fine structure at low temperatures

D. Group at 3.40

E. Group at 2.43

the high Debye temperature (2340°K) of diamond. Making the measurements of the change in absorption with temperature at high temperatures, Collins and Fan were able to produce reliable variations in absorption which agreed with the theoretical expression. The Raman absorption in diamond is at 1332 cm^{-1}, but since the absorption at 2175 cm^{-1} of the strong 4.6μ absorption also corresponded well with the theoretical expression relating lattice elastic constants with the limiting lattice vibration frequency, the existence of combination modes was implied. It appears as if the 2175 cm^{-1} absorption is associated with an optical mode phonon. In diamond a linear electric moment is absent. Therefore Lax and Burnstein (11) proposed that the lattice absorption in diamond must involve charge deformation. They suggested a model whereby one acoustic and one optical phonon are required for photon absorption. The phonons are necessarily of short wavelengths which provide the required assymmetric displacement within the two sublattices of diamond. A theoretical study by Birman (12) indicates there are at least eleven and possibly seventeen different phonon frequencies assigned to diamond.

Photoconducting studies were made by Johnson, et. al. (13) at temperatures ranging from 127°K to 300°K. Photoconductivity observed near the intrinsic absorption energy at about 5.25 ev increases toward shorter wavelengths. Some structure has been observed in the photoconductivity spectrum. In Type IIb diamond at room temperature, maxima occurred at 0.224, 0.228, and 0.68μ. Halperin and Nahum (14) obtained the photoconductive spectrum at wavelengths from 0.20 to 0.23μ. They detected photoconductivity between 1μ and 4μ, but were unable to record the spectrum due to technical difficulties. Hardy,

Smith, and Taylor (15, 16) detected the photoconductivity in Type IIb diamonds at 80°K and on the basis of the response from 1.4 to 3.4μ attempted to correlate the photoconductivity minima with the phonon spectra in diamond. A subsequent examination by Krumme (17) of this laboratory extended the measurements to the spectral range from 0.8 to 5.0μ at temperatures of 77°K and 4.2°K. Again using phonon-photon interactions, he suggested a new and more satisfactory scheme which provided a distinct correlation for up to eight 0.165 ev phonons.

Measurements of the carrier lifetime in diamond indicates the complexity of the problem in diamond. Decay times obtained by Wayland and Leivo (18) for various exciting wavelengths are 9μ sec, 1/4 and 30 sec, and 6, 7, 12, 30, 34, and 84 minutes. The diamonds examined by Wayland and Leivo are included in the diamond collection of the present study.

Hall measurements by Johnson, et. al. verified that the semiconducting diamonds studied in the current investigation are p-type semiconductors, and the mobility for holes is 1300 cm^2/volt-sec. On the basis of a particular model using both donor and acceptor levels, the solutions which gave the best fit to the experimental curve were when the effective hole mass was 0.3 m_e, the acceptor density was 3.25 X 10^{16} atoms per cm^3, and the donor density was 9.5 X 10^{15} atoms per cm^3.

It has been known for many years that some diamonds would luminesce. Crookes observed some diamonds which luminesced when they were rubbed with silk. Halperin and Nahum (14) reported a luminescent recombination process with quite a broad spectral distribution. They showed that the electroluminescent and fluorescent curves are essentially identical. In a study of the thermoluminescent glow curves,

they observed activation energies of 0.22, 0.30, 0.38, 0.52, and 0.7 ev. Wolfe and Woods (19) photographed the electroluminescent spectrum of diamond and showed that the peak intensity occurred at 0.44μ.

Male (20) recorded the luminescent excitation spectrum for three types of diamond. Both Type I and Type IIa diamonds showed bands, whereas, the Type IIb diamond displayed a broad excitation spectrum beginning at 5.25 ev. The maximum occurred at 5.6 ev, and a lesser maximum which is possibly common to all diamond types was found at 5.5 ev. Male and Prior (21) observed the intrinsic recombination radiation in a Type IIa diamond utilizing carrier injection to produce the electron density necessary to make this improbable process measureable. They recorded a strong band at 0.440μ and two weaker bands at 0.413 and 0.425μ.

Krumme and Leivo (22) showed that the temperature dependence of the afterglow of the luminescence was characteristic of phosphorescence rather than slow fluorescence and indicated multiple metastable levels existed. They also reported a red phosphorescence in Type IIb diamond. If a diamond does luminesce, it may be violet, blue, blue-white, green, yellow, orange, or red. In some cases they will luminesce brilliantly.

Electron spin resonance studies indicate that the spin resonance absorption is associated with the acceptor center in p-type diamonds (23). Colored diamonds usually display a complicated spin resonance spectra. The strength of the 8μ infrared absorption in Type I diamond was correlated with electron spin resonance and mass spectroscopic measurements. The concentration of nitrogen was found to vary directly with the absorption of the infrared at 8μ. (24)

Millimeter cyclotron resonance experiments by Rauch (25) on semiconducting diamonds at 1.55°K gave 0.355 ev for the activation energy and 0.006 ev for the spin-orbit splitting energy. He obtained hole effective masses of 2.12, 1.06, and 0.7 for the three valence bands where the last value is for holes in the split-off band.

A recent study of the density of natural diamonds shows that Type IIb semiconducting diamonds are less dense than Type IIa or Type I diamonds (26). This is consistent with the suggestion that lattice vacancies are associated with p-type conductivity in semiconducting diamond.

A large number of important studies have been omitted from this survey, and no suggestion is intended that they are less important. The works which have been discussed were selected as being of particular interest to the present investigation.

CHAPTER II

THEORY OF THE JUNCTION PHOTOVOLTAGE

Band Theory of Solids

The band theory of solids has been very successful in explaining many properties of solids. The theory provides information regarding electron energies in a crystalline material. Details of this discussion can be found in various books on the theory of solids (27, 28). The application of one electron theory wherein Bloch functions are used to obtain solutions to the appropriate Schrödinger equation leads to several results. For each state of an electron in the free atom there exists a band of energies in a crystal, and the width of a band is a function of the overlap of the atomic wave functions. In a nondegenerate band, the number of states is equal to the number N of primitive cells in the crystal. However, two electrons of opposite spin fill each state so that each band contains 2 N electrons. The bands may be separated by a gap of forbidden energies, or they may overlap for some values of the electron wave vector k. The bands corresponding to the atomic valence electrons which have greater overlapping wave functions determine many of the interesting properties of the crystal. If the band of greatest energy which contains any electrons is full of electrons and this band is separated by a forbidden energy gap E_g from the next highest band of energy states, there can be no change in the

electron velocity distribution within the band upon application of an electric field. This crystal is then an insulator. If the band is partly full or if an empty band overlaps a full band, the crystal is a metal.

A semiconductor is defined as a material with a conductivity between that of a metal and an insulator. By applying quantum statistics to a simple model of an electronic semiconductor containing impurities at low temperatures, the charge carriers associated with states within the forbidden gap are found to be liberated in increasing numbers with increasing temperature. This results in decreasing the resistance on increasing the temperature. As the temperature continues to increase, a point is reached where the impurities are unable to add further to the conduction process. There is an increase in the lattice vibrations caused by the rise in temperature. The net result is an increase in resistance with increasing temperature. Finally, as the temperature is increased further, electrons are excited across the energy gap and can cause a reduction in the resistance. These three processes give rise in general to three regions of different slope on a logarithmic plot of resistivity vs temperature for an impure semiconductor. The high and low temperature regions may have negative coefficients, and the intermediate region can have a positive coefficient.

Diamond has three valence bands which have maxima at the center of the Brillouin zone, $k = 0$. Two of the bands are degenerate at $k = 0$, and the third band edge is split off by 0.006 ev due to spin-orbit interaction. The conduction band minima are found near to but not at the edge of the Brillouin zone along the (1,0,0) axes. Since

the conduction band is empty and separated by about 5.5 ev from the valence band, intrinsic diamond is an insulator.

Photovoltage at a Metal to Semiconductor Contact

In order to understand the theory of the photovoltage at a metal to semiconductor contact, the nature of the barrier at the contact must be examined. Most of the metallic contacts to diamond which were examined in this study could be removed with an acid with no apparent alteration of the original diamond surface. Even the metal point contacts did not change the diamond surface detectably. Therefore an explanation of the experiments requires a combination of both the free surface theory of semiconductors and the barrier theory for metal to semiconductor contacts.

In a simplified model, a metal with a work function W_m coming in contact with a p-type semiconductor with work function W_s, produces the sequence of changes shown in Fig. 1, where E_{fm} is the fermi level of the metal, and E_{fs} is the fermi level of the semiconductor. E_{vm} and E_{vs} are the energies at the distance in the vacuum outside the metal and semiconductor respectively where the force due to the image charge of the electron is negligible. E_c is the energy at the bottom of the conduction band, δ is the energy at the center of the forbidden gap, and E_v is the maximum energy of the valence band. The work function of the metal is defined as $W_m = E_{vm} - E_{fm}$. The work function of the semiconductor is defined as $W_s = E_{vs} - E_{fs}$. The subscript "o" indicates those values before contact. As the metal and semiconductor are brought into contact, there is a contact potential difference, φ,

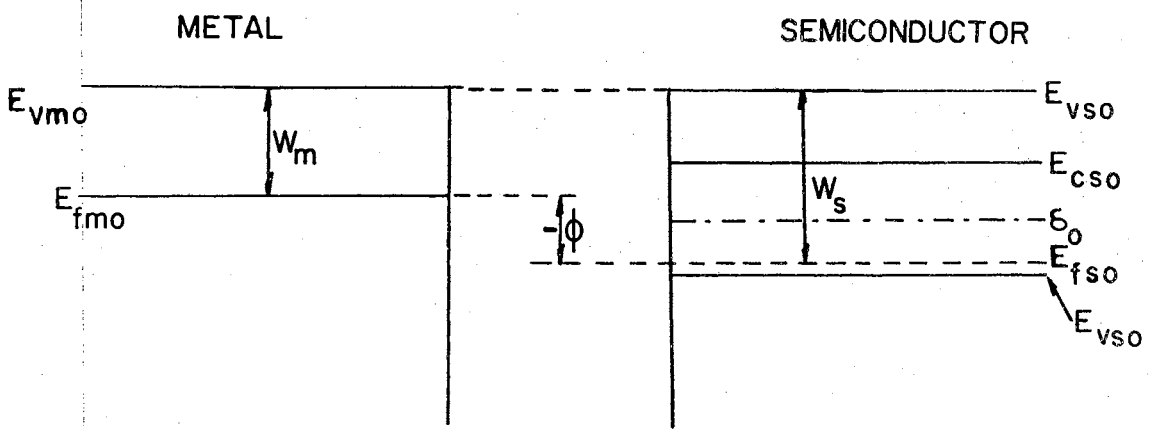

Fig. 1a. The energy band structure before contact of a metal and p-type semiconductor with no surface states.

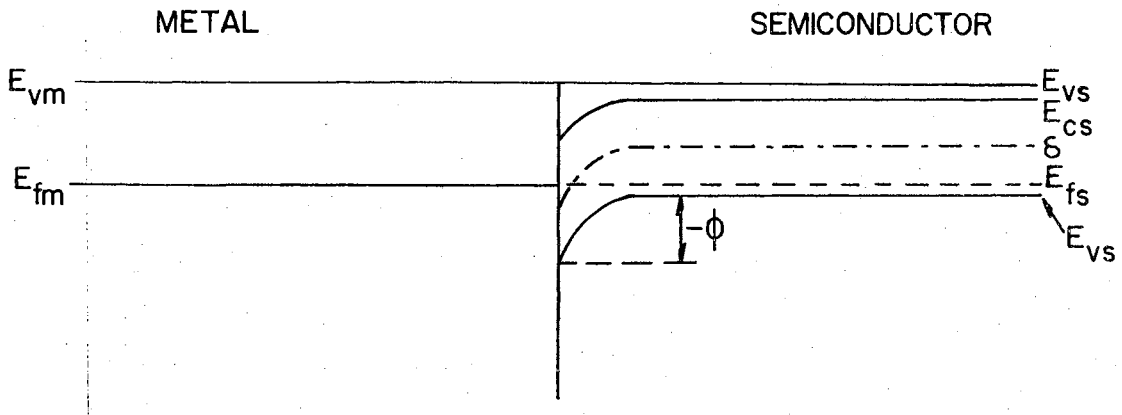

Fig. 1b. The energy band structure at the contact of a metal to p-type semiconductor with no surface states.

where

$$(1) \qquad \varphi_o = W_{mo} - W_{so}.$$

Note that in the case of Fig. 1, the work function of the metal with respect to E_{vs} is relatively unchanged while the work function of the semiconductor with respect to E_{vm} is considerably reduced. When φ has a negative sign, it presents a barrier to holes. When φ has a positive sign it presents a barrier to electrons.

The contact potential difference manifests itself in the case of Fig. 1 through a potential barrier to holes at the metal to semiconductor contact. In this case, the barrier is a dipole layer which consists of a space charge region in the semiconductor and an induced charge on the metal surface. In Fig. 1 there is an increase of electrons in the space charge region and an induced positive charge in the metal surface. If a voltage is applied to the junction, most of the potential drop occurs across the region of highest resistance, the barrier layer. When the potential of the semiconductor is positive with respect to the metal, the electron energy levels of the semiconductor are lowered, and the holes may flow more easily to the metal over the reduced potential hill. This is the direction of easy current flow. On the other hand, if the semiconductor is negative, its levels are raised increasing the height of the hill and making it more difficult for holes to travel from the semiconductor to the metal. This is the direction of high resistance.

This discussion has emphasized the special combination of materials in Fig. 1. Figure 2 shows the other possible combinations of metals and semiconductors which may occur (28). If the barrier is high enough as

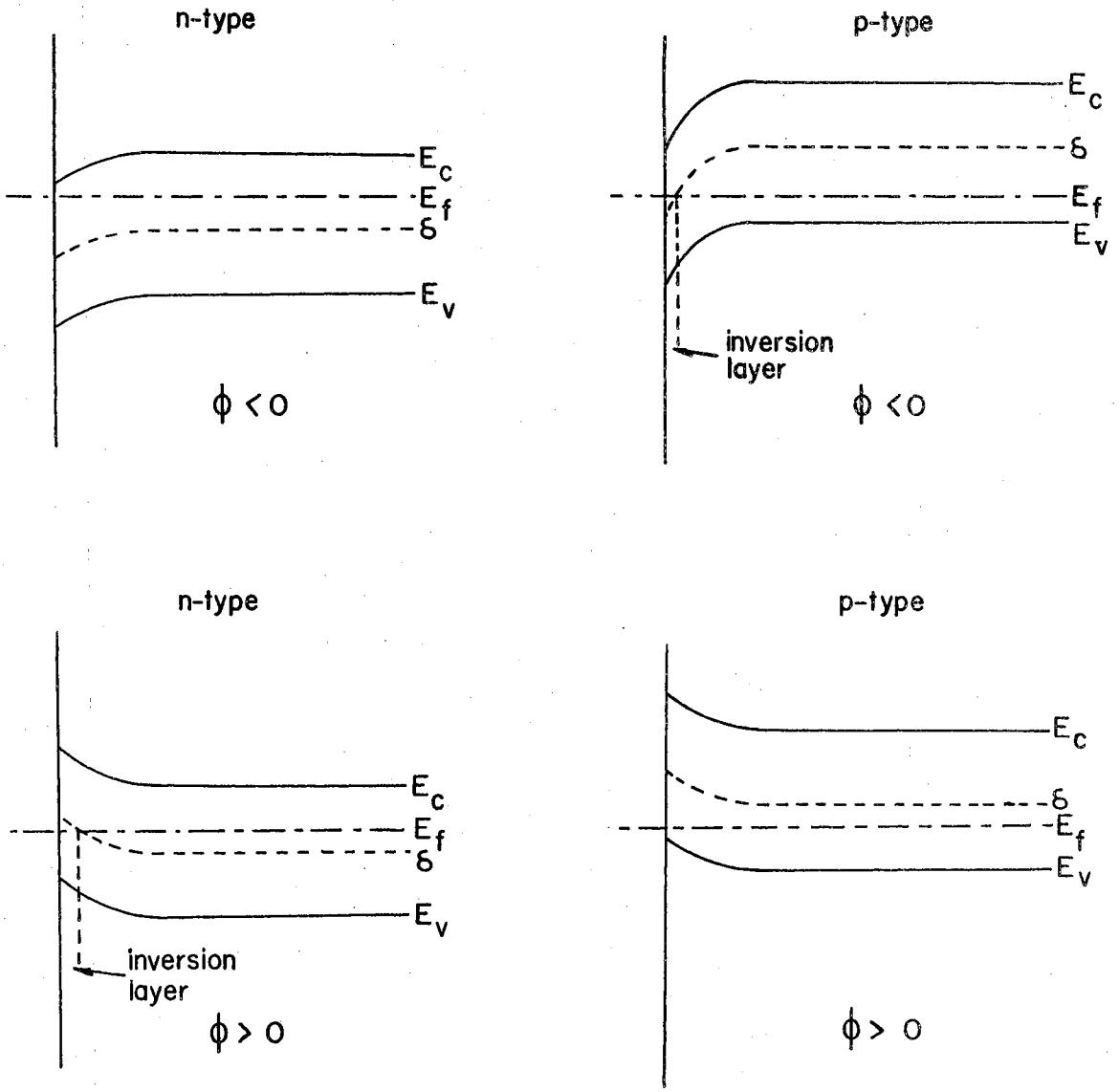

Fig. 2. Possible barriers at a metal to semiconductor contact for both n- and p-type semiconductors.

in Fig. 1, the Fermi level may cross the center of the forbidden gap. When this occurs, a surface inversion layer gives rise to n-type "channels" on the surface of this p-type material. Similarly p-type "channels" may be produced on the surface of n-type material.

Schottky (29) discussed a model for a metallic contact to a semiconductor. Using Poisson's equation:

$$\nabla^2\varphi = -\rho/\epsilon$$

and the potential φ, he found

$$\frac{d^2\varphi}{dx^2} = \frac{N_a q}{\epsilon}.$$

Here q is the positive electron charge, N_a is the number of ionized acceptor atoms per unit volume, and ϵ is the absolute dielectric constant.

Integrating gives

$$\frac{d\varphi}{dx} = \frac{N_a q x}{\epsilon} + C_1.$$

Herein lies a difficulty with this model. What should be the value of

$$\left[\frac{d\varphi}{dx}\right]_{x=0}?$$

Generally it is assumed to be zero. Thus,

$$\frac{d\varphi}{dx} = \frac{N_a q x}{\epsilon}$$

and integrating again gives

$$\varphi = \frac{N_a q x^2}{2\epsilon} + C_2$$

Since $\varphi \equiv 0$ at $x = 0$, $C_2 = 0$ and

$$\varphi = \frac{N_a q x^2}{2\epsilon}$$

and the thickness of the barrier, d, is

$$d = \left[\frac{2\varphi\epsilon}{N_a q}\right]^{\frac{1}{2}}$$

To obtain the current-voltage relationship at an n-type semiconductor to metal contact, first consider an element of 6-dimensional phase space $d\Phi$. The number of electrons in the element of phase space of the metal is $2f d\Phi$ where f is the Fermi-Dirac distribution function:

$$f = \frac{1}{e^{(E-E_f)/kT} + 1}$$

where $E = \frac{m}{2}(\xi^2 + \eta^2 + \zeta^2)$, k is Boltzmann's constant, T is the absolute temperature, and E_f is the Fermi level. The factor 2 is necessary since each state may hold two electrons with opposite spins. Define $\hbar$ to be Plank's constant divided by 2π and assume the thermal energy of an electron inside the barrier is negligible relative to the energy it gains from the electric field over a distance comparable to one mean free path. Since each cell with a volume of $\hbar^3$ in the 6-dimensional phase space corresponds to one state, then the number dn of electrons per unit volume with velocities between the limits ξ,η,ζ, and $\xi + d\xi$, $\eta + d\eta$, and $\zeta + d\zeta$ is

$$dn = 2\left[\frac{m}{\hbar}\right]^3 f . d\xi d\eta d\zeta .$$

If N_{ms} is defined as the number of electrons per unit volume crossing the contact barrier per unit area per unit time from the metal into the semiconductor, then:

$$N_{ms} = 2\left[\, m/\hbar \,\right]^3 \int_0^\infty \int_0^\infty \int_{\sqrt{2\varphi_m/m}}^\infty \frac{\xi \, d\xi \, d\eta \, d\zeta}{e^{(E-E_f)/kT} + 1}$$

where φ_m is the height of the potential barrier in units of electron volts. The barrier is shown in Fig. 3.

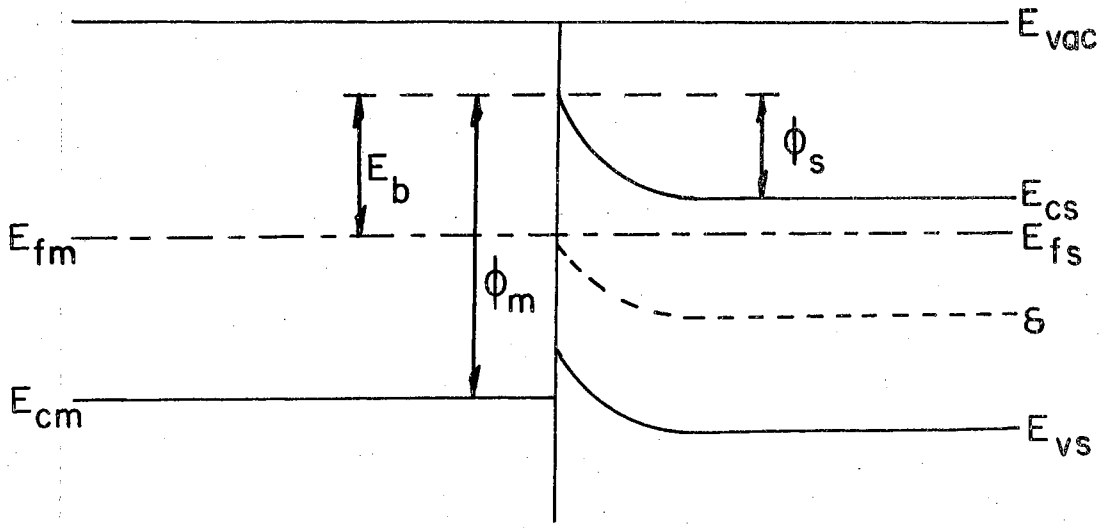

Fig. 3. The barrier at a metal to n-type semiconductor contact with $\varphi > 0$ but no surface inversion layer.

Assuming

$$(E - E_f) \gg kT$$

then

$$N_{ms} \approx \int_0^\infty \int_0^\infty \int_{\sqrt{2\varphi_m/m}}^\infty \left[2(m/\hbar)^3 \, e^{E_f/kT} \right] \xi \, e^{-m(\xi^2+\eta^2+\zeta^2)/2kT}$$

$$N_{ms} = \int_{\sqrt{2\varphi_m/m}}^{\infty} 2(m/\hbar)^3 \, (\pi kT/2m) \, e^{E_f/kT} \, \xi \, e^{-m\xi^2/2kT} \, d\xi$$

$$N_{ms} = -\left[(m/\hbar)^3 \, (\pi kT/2m) \, e^{E_f/kT} \right] (2kT/m) \, e^{-m\xi^2/2kT} \Big\}_{\sqrt{2\varphi_m/m}}^{\infty}$$

Therefore,

$$N_{ms} = \frac{m\pi k^2}{\hbar^3} \cdot T^2 \cdot e^{(E_f - \varphi_m)/kT} = A \cdot T^2 \cdot e^{-qEb/kT}$$

where E_b is the height of the electrostatic potential barrier above the Fermi level as measured in volts, and q is the charge of the electron. A similar calculation of the number of electrons N_{sm} per unit volume moving across a unit area of the barrier from the semiconductor to the metal in a unit time yields the solution

$$N_{sm} = AT^2 e^{q(E_f - \varphi')/kT}$$

where

$$\varphi' = \varphi_s - V$$

and V is the voltage applied to the contact.

Thus

$$N_{sm} = AT^2 e^{q(V - E_b)/kT}.$$

The current density j is defined by

$$j = Nqv$$

where N is the electron density, v is the velocity, and the total current density j is the sum of the currents across the barrier.

$$j = A'T^2 e^{q(V - E_b)/kT} - A'T^2 e^{-qE_b/kT}$$

where $A' = Aqv$

$$j = A'T^2 e^{-qE_b/kT} (e^{qV/kT} - 1) = j_o(e^{qV/kT} - 1).$$

The last equation is called the diode equation. In terms of total current across a plain barrier the diode equation is

$$i = I_o(e^{qV/kT} - 1)$$

where $$I_o = (\text{Const})T^2 e^{-qE_b/kT}.$$

Here i is the net current flowing through the circuit and I_o is the reverse saturation current. The graphic significance of the diode equation is shown in Fig. 4.

Experiments have usually required that I_o be fitted from laboratory data (30). In fact, the theoretical and experimental I_o may differ by many orders of magnitude. Additional factors, α and β, are frequently found to be necessary in order to adjust the mathematical description to fit experimental data. Therefore the relation that usually satisfies experiments is:

$$i = I_o \left[(1 + \alpha)e^{\beta qV/kT} - 1\right] \quad (31).$$

These deviations can be attributed to several causes. Since the description of the potential barrier near the metal is not clear, the slope was arbitrarily taken as zero. The surface of the semiconductor is known to contain permitted energy states that are different from those of the bulk and which can be attributed to both inherent crystal properties and variations due to external influences. Finally, the diode equation was derived under the assumption that the injected majority carrier density was small compared to the equilibrium value, and therefore did not change the nature of the potential barrier at equilibrium.

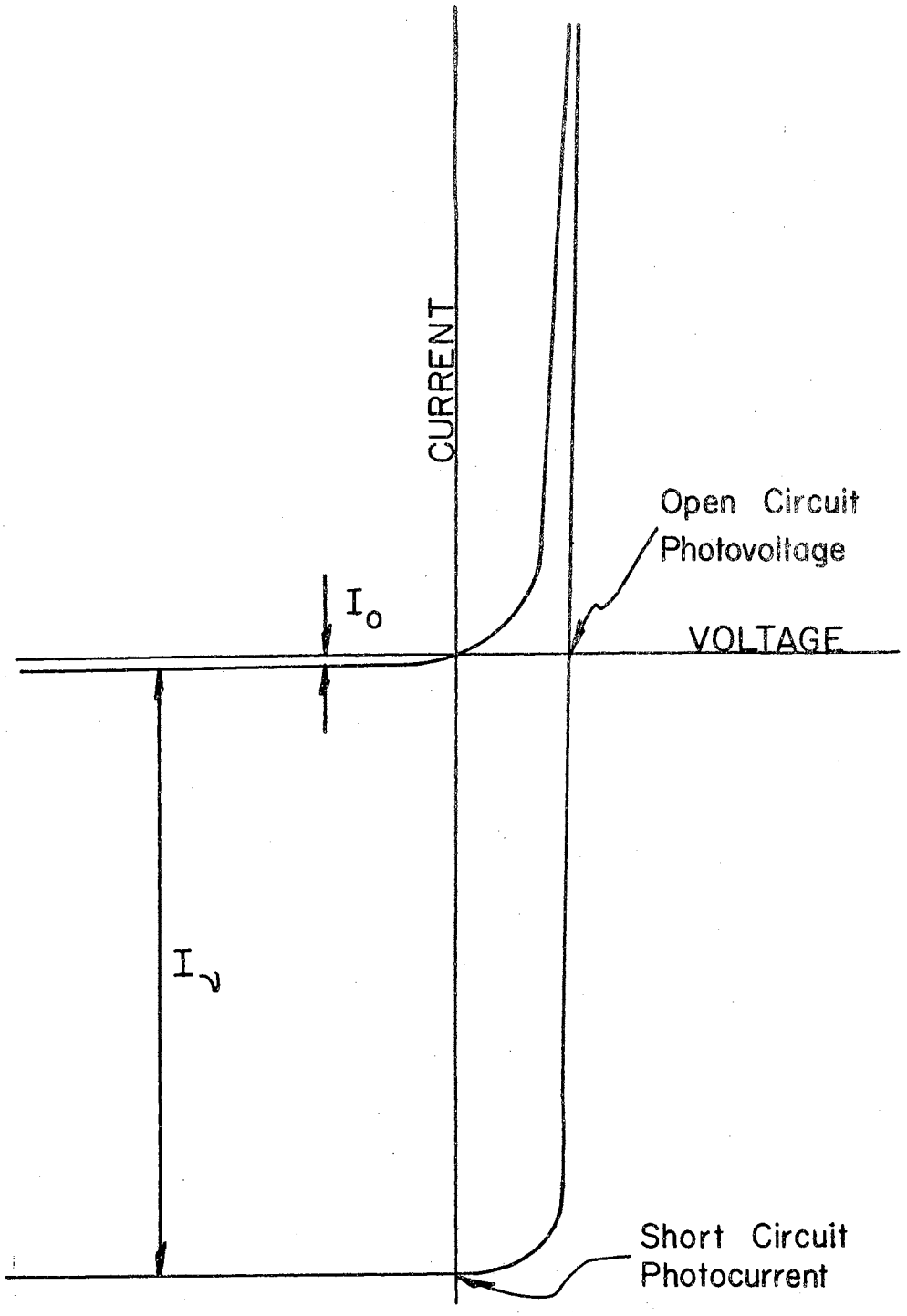

Fig. 4. Graphical representation of the photodiode equation.

In the simplified model presented above no mention of surface states was made. Bardeen (32) corrected the simplified model by elaborating on Tamm's surface states and considering both a surface and bulk charge.

The inclusion of states characteristic of the surface results in a redistribution of the charges and the establishment of barriers at the surface of the semiconductor even when it is not in contact with a metal. The presence of surface states may be considered reasonable due to such things as the presence of foreign surface atoms, broken crystal bonds at the surface, and the rapid change in bulk potential as the surface is approached. Recent computations of permitted energy levels indicate that the levels in the valence band shift toward the center of the forbidden gap as the diamond surface is approached (33).

The surface states can usually be separated into two classes (31). The first class has states of a relatively large density (approximately 10^{12} or more states per square centimeter in germanium). These states are called "slow" states because they exchange charge very slowly with the bulk material. The time constant of charge exchange are normally measured in seconds or tenths of seconds. These states are strongly affected by the ambient atmosphere and supposedly exist on or within the composite layer covering the semiconductor surface. This layer is formed by an interaction with the surrounding atmosphere. Little is known about the density or energy distribution of the slow states.

The second type of surface state is called "fast" because these states and the bulk material can exchange charge with time constants of the order of microseconds. The fast states are supposedly located at or near the interface between the bulk and the surface layer and are apparently unaffected by the atmospheric ambient. These states are relatively less numerous (approximately 10^{11} or less states per square centimeter in germanium) than the slow states and may play a smaller role in determining the surface potential. Both discrete and continuous distributions of energy levels have been found for the fast states in semiconductors.

The distinction between fast and slow states usually is a clear-cut one, but this has not always been the case. For example, slow states have been observed with time constants of 10^{-3} sec. An additional effect of the surface states is observed when non-interrupted light is incident on the crystal surface. The photo-voltage reaches a maximum soon after the onset of illumination and then decays to zero. This has been interpreted as being due to the charge accumulating in the slow states and compensating the inner charge. When the illumination ceases, a signal of reverse polarity appears corresponding to discharging of the slow states. Relaxation times are generally of the order of tens of seconds or minutes.

Thus with the presence of surface states, the barrier of the metal to semiconductor contact will not be expected to be as sensitive to the type of metal at the contact. Many of the properties of the contact can still be described satisfactorily with modifications to allow for the surface states. A typical example of this is

the variation of the photovoltage with intensity of illumination. If the rate of generation of carriers is assumed to be proportional to the intensity of illumination, the additional photocurrent I_ν is included in the diode equation by

$$i = I_o\left[(1 + \alpha)\ e^{\beta qV/kT} - 1\right] - I_\nu$$

where i is the total current. Figure 4 shows the graphic behavior of this equation. α is chosen such that as $I_\nu \to \infty$, $I_o(1 + \alpha) \to \Gamma I_\nu$ where Γ is a constant. Also α has the property that as $I_\nu \to 0$, $\alpha \to 0$. If i = 0, the open circuit photovoltage V_m is then found from

$$V_m = \lim_{I_\nu \to \infty} \frac{kT}{\beta q} \ln\left[\frac{I_\nu - I_o}{I_o(1+\alpha)}\right] = \frac{kT}{\beta q} \ln \frac{I_\nu}{\Gamma I_\nu} = \frac{kT}{\beta q} \ln \frac{1}{\Gamma}$$

This relation indicates a saturation of the photovoltage on increased illumination, and a similar saturation is observed experimentally. The maximum photovoltage is suggested by the diagram in Fig. 5. As light shines on the contact, electrons generated in the semiconductor "fall" down the potential hill to the metal while the holes are repulsed into the bulk of the semiconductor. This action results in forward biasing the contact and can continue until the photovoltage approaches the barrier height. If the photovoltage equaled the potential barrier height, there would no longer be a potential barrier that could separate the charge. This separation of the charges is of course a prerequisite for the photovoltage.

The saturation of the photovoltage with increased illumination poses a serious consideration while observing the photovoltaic response at a junction. For example, when examining the spectral response of the photovoltage at a junction, care should be taken

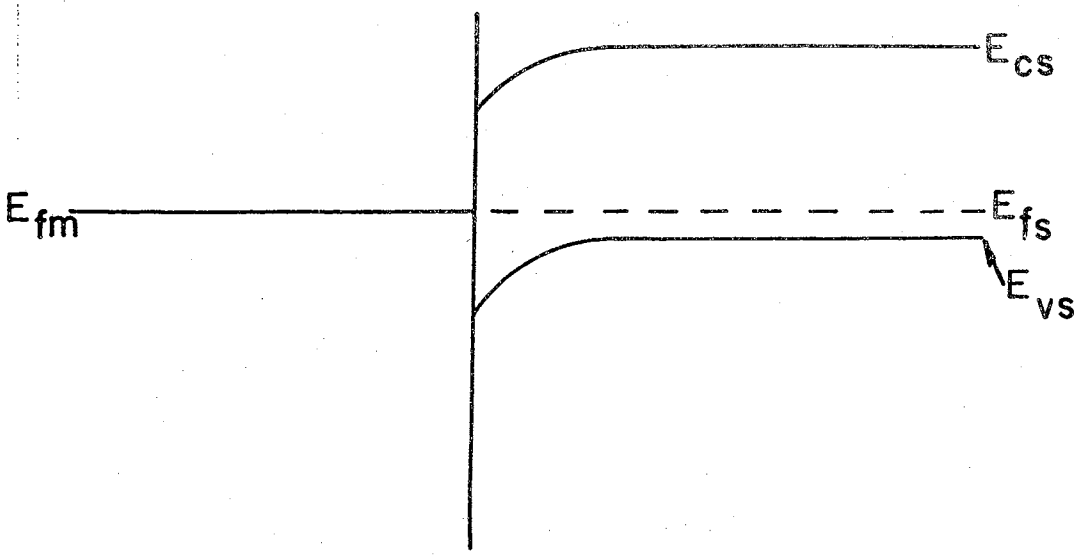

Fig. 5a. A metal to p-type semiconductor contact before irradiation with light.

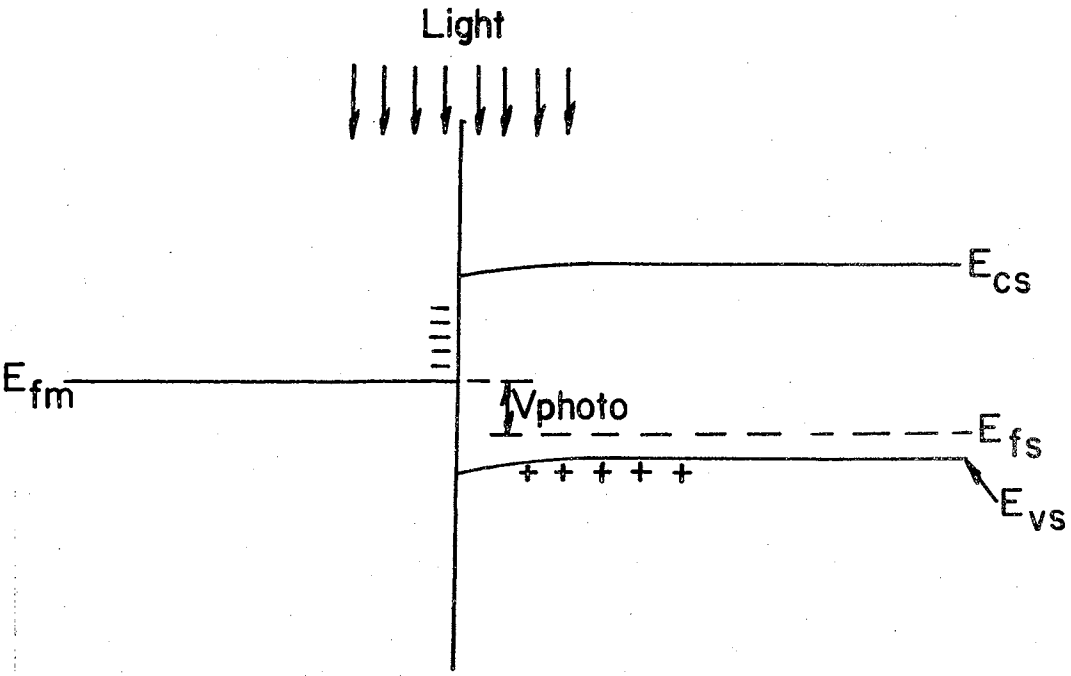

Fig. 5b. A metal to p-type semiconductor contact before irradiation after light.

to insure that the photovoltage is proportional to the incident photon flux. Otherwise tedious data reduction will be necessary in order to relate the incident wavelength with the photovoltage spectral sensitivity.

The spectral response of the photovoltage can give information about the width of the energy gap, intermediate states in the energy gap near the junction, and phonon assisted transitions across the energy gap. As the energy of the photon is increased it finally becomes large enough to excite electrons across the energy gap. Since the process becomes highly probable for photons of this energy, the optical absorption is very high and takes place near the surface on which the photons are incident. The photovoltage per photon per second is then very high, and the photon's energy is a measure of the energy gap of the semiconductor. At higher temperatures phonons may assist in the electron's transition across the gap, and therefore a photon with an energy less than that of the energy gap may succeed in creating a hole-electron pair. As the temperature is reduced, the number of high energy phonons is reduced, and the spectral response shows a more abrupt change at the energy of the semiconductor's energy band gap. An additional effect to be included in the spectral response is the observation of an increase in energy band gap with decreasing temperature. Therefore, as the temperature is decreased, the spectral response may show an additional shifting to shorter wavelengths of the photovoltage per photon per second peak corresponding to electron transitions across an increased energy gap. As in Fig. 1, excitation of an electron from the

valence band to a state intermediate in the gap but located at the surface, will cause the hole to be repelled into the bulk. This separation of charge may give rise to a photovoltage, and be observed in the spectral response of the photovoltage.

Finally, an account must also be taken of the Dember potential. The Dember potential is established by the carriers having different diffusion rates. A separation of charges results when a carrier of one charge is able to diffuse away faster than the oppositely charged carrier. The Dember field acts to equalize the flow rates of holes and electrons away from the region of illumination. This field always acts to slow down the diffusion of the most mobile carrier and is at most a few kT/e units. Thus the Dember potential can usually be disregarded.

Circuit Analysis of Photovoltage Measurements

Most photovoltage measurements result in the same equivalent circuit. The circuit used to measure a photovoltage has a direct influence on the photovoltage and must be analyzed in order to interpret the results of the measurements. The equivalent circuit for the photovoltage measurements is shown in Fig. 6. Here the irradiated junction is shown as a constant current generator i_ν with a nonlinear impedance R_j, an internal series resistance R_s, and an internal shunt resistance R_{sh}. An external current i_L may flow through the measuring device which has a load resistance R_L and therefore indicates a voltage V_L. The photovoltage V is given by the equations

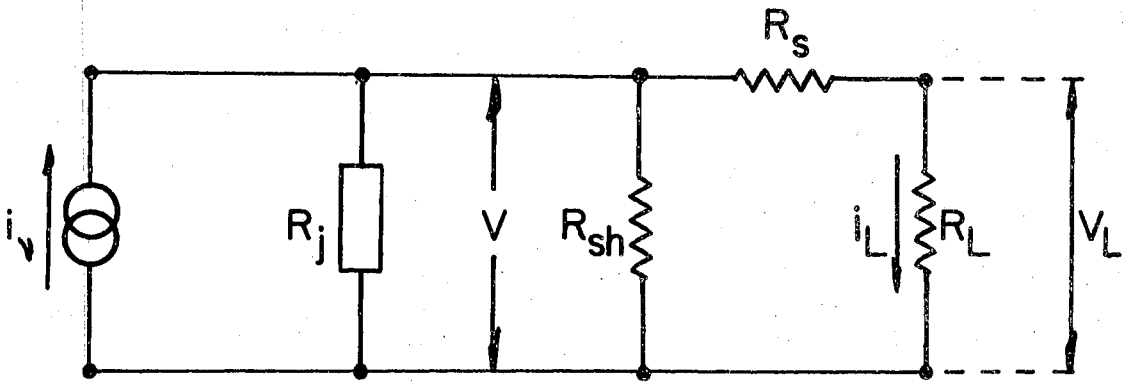

Fig. 6. The equivalent circuit for photovoltage measurements.

$$V_L = V - i_L R_s$$

and

$$i_L = I_o \left[(1 + \alpha) e^{\beta q V / k\Gamma} - 1 \right] + \frac{V}{R_{sh}} - i_\nu$$

Experimentally, R_{sh} is found to be extremely large and can usually be neglected.

In order to measure the open circuit photovoltage, R_L should have an infinite value, but in practice where the photovoltage is varying with time, an electrometer with a very large input resistance may be used to approximate the open circuit photovoltage. As long as R_s, the resistance of the semiconductor bulk, is small compared with R_L, $i \approx 0$, $iR_s \approx 0$ and $V \approx V_L$.

However, as the temperature is reduced, R_s increases and may approach R_L. When the temperature is decreased even further and

$R_s \gg R_L$, most of the photovoltage is dropped across R_s, and the electrometer only indicates a fraction of the true photovoltage. Consequently R_s should be kept much smaller than R_L, and where this is impossible, the above considerations must be noted. This effect will be discussed further in Chapter IV.

CHAPTER III

EXPERIMENTAL PROCEDURES AND RESULTS

The Diamond Collection

A diamond collection of seventy-four diamonds was examined in this study. All of the specimens are natural diamonds and the geographic origins of only several are known. However, from their physical description, the sources of a number of them such as the "Congo cubes" are suspected. Experimenters that are confined to examining natural specimens of generally unknown origins and histories are familiar with the need to include at least several samples in their investigations. Investigators of diamond thus need a large number of samples for meaningful results, but must temper their enthusiasm with considerations for the time required for investigations, the difficulty in finding suitable specimens, and of course the money needed to establish an extensive diamond collection. Once a suitable collection is established, the wide variations in the diamonds require an extensive initial study to catagorize them and record any unusual behavior. Table 2 shows the results of such a study on the diamonds examined in the present investigation. These results will help to display the correlations that are discussed in Chapter IV. Figures 7 and 8 show how the physical characteristics of the diamonds varied. Diamond chips, diamonds found naturally as cubes and as triangular flats, and

TABLE II

SUMMARY OF PROPERTIES FOR THE DIAMONDS EXAMINED

#	Type	Description	Wt. (gm)	Luminescence F	Luminescence P	Optical Cut-off (mμ)	Infrared Absorption (μ) 6.55	3.56	7.8	8.2	7.3	7.05	Photo-conductivity	Photo-voltage
1	IIa	Pale yellow	.1094	W-Y	yes	225	ND	ND	VW	ND	VW	ND	W	VS
2	I	White triangle	.0941	W-R	yes	300	VW	ND	VVS	VVS	S	ND	VW	W
3	I	White, two flat faces	.0772	W-B	yes	307	VW	ND	VVS	VVS	VS	VVW	W	M
4	I-IIa	White tumble stone	.0739	W-B	yes	293	ND	ND	VVS	VS	VS	ND	W	VW
5	I	White triangle with two dark yellow sides	.1044	W-V	yes	300	ND	ND	VVS	S	S	ND	W	M
6	I-IIa	White chip	.0753	W-B	yes	291	VW	ND	VVS	S	S	ND	VW	W
7	I-IIa	White triangle	.0646	M-B	yes	236	ND	ND	VW	W	VW	ND	ND	W
8	I-IIa	Very pale yellow green triangle	.0686	W-RY	yes	289	ND	ND	VS	S	S	ND	W	W
9	IIa	Very very pale brown triangle	.0708	W-Y	yes	228	ND	ND	VVW	VVW	VVW	ND	S	S
10	I-IIa	White triangle	.0804	W-Y	yes	293	ND	ND	VS	VS	S	ND	S	S

TABLE II (Continued)

#	Type	Description	Wt. (gm)	Luminescence F	P	Optical Cut-off ($m\mu$)	Infrared Absorption (μ) 6.55	3.56	7.8	8.2	7.3	7.05	Photo-conductivity	Photo-voltage
11	IIa	White triangle	.0666	W-G	yes	226	ND	ND	VW	VW	W	ND	S	VVS
12	I-IIa	Cloudy white triangle	.0684	W-Y	yes	284	ND	ND	VS	S	S	ND	W	M
13	I-IIa	Pale yellow, two flat faces	.0552	S-B	yes	289	W	ND	VVS	VVS	VS	W	ND	S
14	I-IIa	White triangle	.0528	W-R	yes	295	VW	ND	VVS	VVS	VS	ND	ND	W
15	I-IIa	White triangle	.0612	W-R	yes	274	VW	ND	VVS	VVS	VS	ND	W	W
16	I	Very very pale brown trapazoid	.0650	W-Y	yes	300	ND	ND	VS	S	S	ND	W	M
17	I	Crushed	.0551	S	yes	305				W	ND			
18	I-IIa	Very pale green trapazoid	.0541	S-B	yes	289	VW	ND	VVS	VS	VVS	W	VW	W
19	I-IIa	White triangular	.0543	W-Y	yes	271	ND	ND	VS	S	S	ND	S	M
20	I-IIa	White triangle	.0410	M-B	yes	280	ND	ND	S	S	S	VW	W	W
21	IIa	White trapazoid	.0337	W-Y	yes	225	ND	ND	VW	VW	VVW	ND	ND	S
22	I-IIa	Very very pale green triangular tumble stone	.0436	S-B	yes	285	ND	ND	S	S	S	VW	W	W

TABLE II (Continued)

#	Type	Description	Wt. (gm)	Luminescence F	Luminescence P	Optical Cut-off ($m\mu$)	Infrared Absorption 6.55	3.56	7.8	8.2	7.3	7.05	Photo-conductivity	Photo-voltage
23	I-IIa	Very very pale green trapazoid	.0491	VW-B	yes	293	ND	ND	VVS	VS	S	ND	W	VW
24	I	Very pale yellow triangle	.0483	VW-Y	yes	300	ND	ND	S	W	W	ND	W	M
25	I-IIa	White triangle	.0398	M-B	yes	286	ND	ND	VS	VS	VS	VW	W	W
26	I	Very pale gray	.0418	W-B	yes	301	ND	ND	VVS	VS	S	VW	W	W
27	I	Very very pale gray triangle	.0383	W-R	yes	300	ND	ND	VVS	VS	W	ND	S	M
28	I	Very pale yellow triangle	.0414	M-R	yes	312	W	ND	VVS	VVS	S	W	VW	W
29	IIa-I	Very pale yellow triangular tumble stone	.0359	M-Y	yes	238	ND	ND	W	W	W	ND	W	M
30	I	Crushed	.0311		yes	303								
31	I	Very pale yellow triangle	.0452	W-RY	yes	304	W	ND	VVS	VVS	VS	W	VW	W
32	I-IIa	Very pale brown triangle tumble stone	.0306	VW-Y	yes	270	ND	ND	S	S	S	ND	S	VVS
33	I-IIa	White triangle	.0360	M-B	yes	282	ND	ND	S	W	VW	ND	W	W

TABLE II (Continued)

#	Type	Description	Wt. (gm)	Luminescence F	Luminescence P	Optical Cut-off ($m\mu$)	Infrared Absorption (μ) 6.55	3.56	7.8	8.2	7.3	7.05	Photo-conductivity	Photo-voltage
34	I	White triangle	.0357	M-R	yes	307	VW	ND	VVS	VVS	S	W	VW	W
35	I-IIa	Crushed	.0314	S	yes	294								
36	I	Very pale gray triangle	.0368	W-RY	yes	308	W	ND	VVS	VVS	VS	VW	W	M
37	I-IIa	Very pale yellow triangle	.0282	W-Y	yes	277	ND	ND	S	W	W	ND	W	S
38	I-IIa	Very pale brown triangle	.0204	VVW-Y	yes	285	ND	ND	VS	S	S	ND	ND	VW
39	IIa	White, cloudy around rim triangular tumble stone	.0223	M-Y	yes	225	ND	ND	ND	VW	VW	ND	VW	W
40	I-IIa	White triangle	.0290	VW-YG	yes	285	ND	ND	VS	S	S	ND	W	W
41	IIa	White triangle	.0296	W-G	yes	228	ND	ND	VW	W	ND	ND	S	S
42	IIa	Very pale brown two flat faces	.0266	M-RY	yes	227	ND	ND	VW	VW	ND	ND	W	S
43	I-IIa	White triangle	.0295	VS-B	yes	293	ND	ND	VVS	VS	S	W	VW	W
44	IIa-I	White, two flat faces	.0257	W-RY	yes	257	ND	ND	S	W	VW	ND	W	S

TABLE II (Continued)

#	Type	Description	Wt. (gm)	Luminescence F	Luminescence P	Optical Cut-off ($m\mu$)	Infrared Absorption (μ) 6.55	3.56	7.8	8.2	7.3	7.05	Photo-conductivity	Photo-voltage
45	IIa	Very pale brown triangle	.0274	W-Y	yes	230	ND	ND	W	VW	VW	ND	W	M
46	I-IIa	Very pale yellow triangular tumble stone	.0250	S-B	yes	290	W	ND	VVS	VVS	VVS	W	VS	VS
47	IIa	White triangle	.0259	W-Y	yes	226	ND	ND	VVW	VVW	ND	ND	W	M
48	IIa	Very very pale yellow triangle	.0260	VS-Y	yes	232	ND	ND	VVW	VVW	VVW	ND	S	VS
49	I	White triangle	.0225	W-R	yes	301	ND	ND	VVS	VS	S	ND	W	M
50-A	I	Medium yellow flat face	0.0538	W-RY	yes	300	S	ND	VVS	VVS	VVS	S	VS	VW
50-B	I	Medium yellow, two flat faces	0.0660	M-RY	yes	305	S	ND	VVS	VVS	VVS	S	W	VW
51-A	I-IIa	Very pale yellow, one flat face	0.0420	VVS-RY	yes	280	ND	ND	S	S	VW	VVW	S	S
51-B	I-IIa	Pale yellow, two flat faces	0.1143	VVS-RY	yes	280	ND	ND	S	ND	W	ND	S	S
52-A	I	White pyramid	0.0570	VW-G	yes	307	S	ND	VVS	VVS	VVS	W	W	M

TABLE II (Continued)

#	Type	Description	Wt. (gm)	Luminescence F	Luminescence P	Optical Cut-off ($m\mu$)	Infrared Absorption (μ) 6.55	3.56	7.8	8.2	7.3	7.05	Photo-conductivity	Photo-voltage
52-B	I	White parallel pyramid	0.1268	VW-G	yes	307	S	ND	VVS	VVS	VVS	W	ND	W
53-A		Crushed												
53-B	I	Bright yellow, two flat faces	0.0427	S-BR	yes	310	W	ND	VVS	VVS	S	VW	VW	VW
54-A	I-IIa	Dark brown "Bullet"	0.0847	W-RY	yes	292	ND	ND	VVS	VS	VS	ND	ND	VW
54-B	I-IIa	Dark brown, three flat faces	0.0449	W-RY	yes	282	ND	ND	S	S	S	VVW	VW	VW
55	I-IIa	Large dark green arrow heat	0.2329	S-BG	yes	275	VVW	ND	VVS	VVS	VVS	W	VW	M
56	I-IIa	Dark green "spear head" tumble stone	0.0583	S-V	yes	275	ND	ND	S	S	S	ND	VW	M
57	I	Medium green tumble stone	0.0418	M-B	yes	300	ND	ND	VVS	VVS	VVS	W	W	M
58	I-IIa	Dark yellow green "lump"	0.1455	VVS-RY	yes	290	ND	ND	VVS	VS	W	W	VW	VW

TABLE II (Continued)

#	Type	Description	Wt. (gm)	Luminescence F	Luminescence P	Optical Cut-off (mμ)	Infrared Absorption (μ) 6.55	3.56	7.8	8.2	7.3	7.05	Photo-conductivity	Photo-voltage
59	I-IIa	Dark yellow tumble stone	0.0429	VVS-YG	yes	280	ND	ND	S	S	S	W	VW	VW
60	I-IIa	Dark brown tumble stone	0.0472	W-Y	yes	290	ND	ND	VVS	VVS	VVS	W	VW	VW
61	I-IIa	Dark brown, two flat faces	0.0539	W-B	yes	290	VVW	ND	VVS	VVS	VVS	W	ND	VW
62	I	Bright yellow cube	0.0124	W-RY	yes	340	VW	ND	VVS	VVS	VW	S	ND	VW
63	I	Dark yellow brown cube	0.0211	W-Y	yes	350	VW	ND	VVS	VVS	VW	W	VW	VW
64	I	Dark yellow brown cube	0.0175	W-G	yes	350	VW	ND	VVS	VVS	W	S	ND	W
65	I	dark brown yellow cube	0.0229	S-R	yes	350	VW	ND	S	VVS	ND	W	VW	W
66	I	Dark brown yellow cube	0.0356	VW-G	yes	350	VW	ND	VVS	VVS	VVS	VS	ND	M
67	I-IIa	Pale yellow "lump"	0.1780	VVS-Y	yes	295	ND	ND	VVS	VS	VS	VW	W	W

TABLE II (Continued)

#	Type	Description	Wt. (gm)	Luminescence F	Luminescence P	Optical Cut-off (mμ)	Infrared Absorption (μ) 6.55	3.56	7.8	8.2	7.3	7.05	Photo-conductivity	Photo-voltage
DS-1	IIb	Chip, long needle, dark blue	0.0787	W-BW	yes	225	ND	S	ND	ND	ND	ND	VS	VVS
DS-2	IIb	Rectangular parallelpiped blue on one end	0.1726	W-BW	yes	225	ND	S	VVW	ND	ND	ND	VS	VVS
DS-3	IIb	Large dark blue marqui	0.1130	W-BW	yes	230	ND	S	VVW	ND	ND	ND	ND	VS
DS-4	IIb													
DS-5	IIb	Dark blue, two large parallel faces	0.7375	W-BW	yes	230	ND	VS	VW	ND	ND	ND	ND	VVS
DS-6	IIb	Small dark blue marqui	0.0175	W-BW	yes	230	VVW	VS	ND	ND	ND	ND	ND	VS

LIST OF SYMBOLS

Luminescence at 300°K using Mercury vapor black light

Relative Strengths

ND....not detectable
VW....very weak
W.....weak
M.....medium
S.....strong
VS....very strong
VVS...very very strong

Color

R.....red
RY....orange
Y.....yellow
YG....yellow green
G.....green
B.....blue
V.....violet

TABLE II (Continued)

Infrared absorption at 300°K

ND....not detectable
VVW...detectable but less than 4% absorption
VW....5-9%
W.....10-15%
S.....16-40%
VS....41-80%
VVS...greater than 80%

Photoconductivity at 300°K using a tungsten lamp

ND....not detectable
VW....detectable but resistance greater than 0.8 of the original resistance
W.....0.79-0.5 of the original resistance
S.....0.49-0.1 of the original resistance
VS....0.09 of the original resistance or less

Photovoltage at 300°K using a mercury vapor black light

VW....detectable but less than 0.3 millivolts (mv)
W.....0.31 - 0.5 mv
M.....0.51 - 10. mv
S.....00.1 - 50. mv
VS....50.1 - 200. mv
VVS...greater than 200 mv

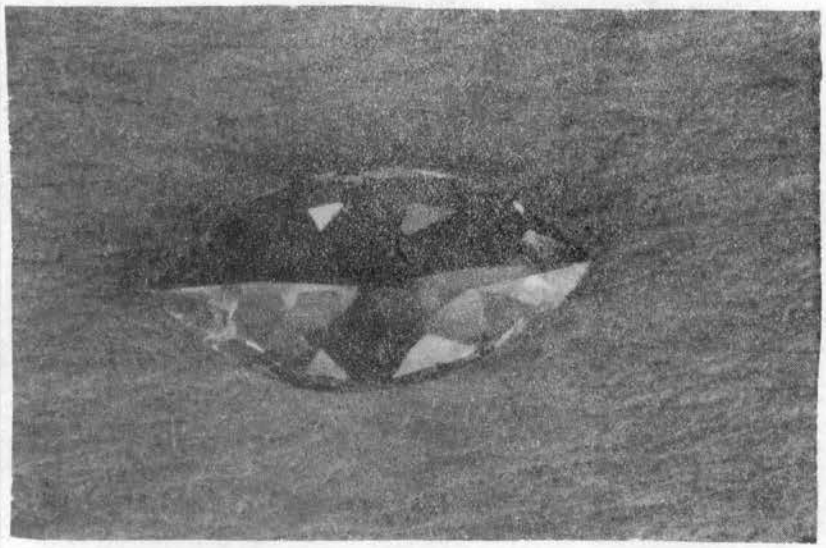

Fig. 7a. A marqui cut Type IIb diamond (DS-3).

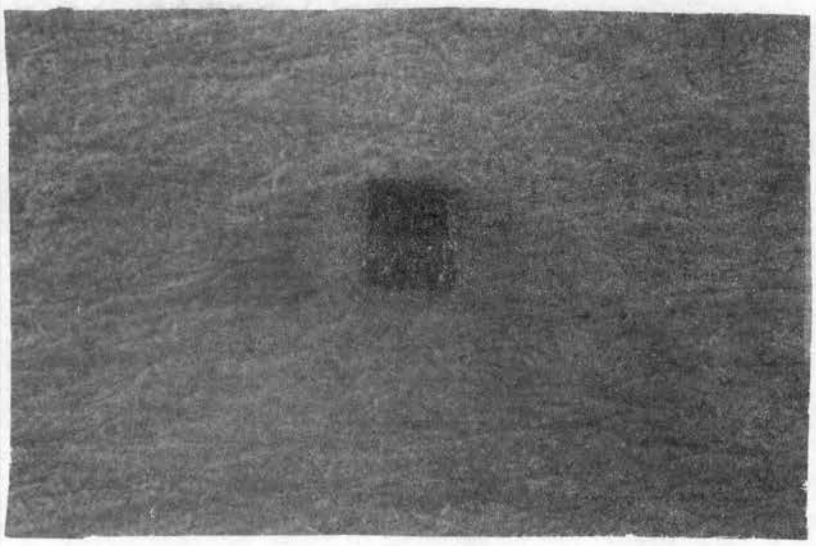

Fig. 7b. A Congo cube Type I diamond (D-63).

Fig. 8a. A large Type IIb diamond (DS-5).

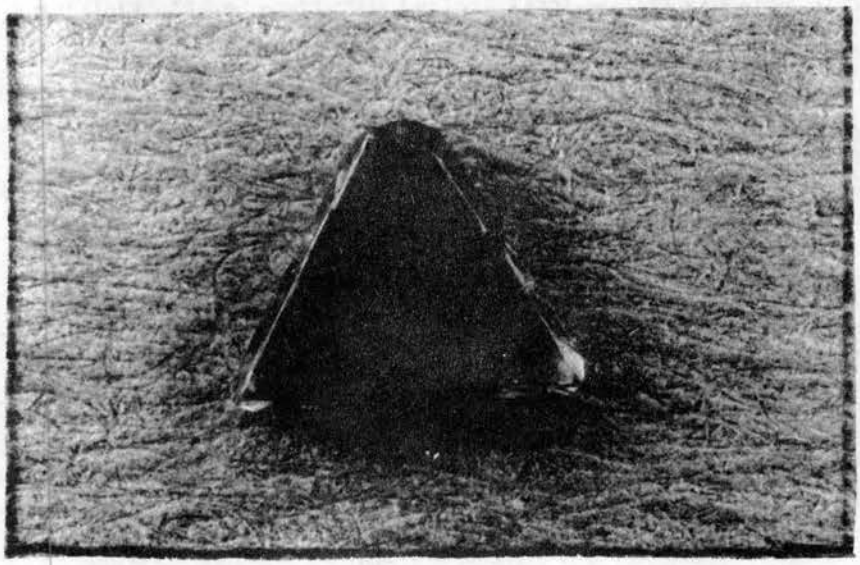

Fig. 8b. A Type IIa triangular flat with carbon inclusions (D-1).

diamonds which have been cut and polished are included in the diamond collection examined. Some of the diamonds were clear or white. Most were colored either yellow, green, brown or blue. Some of the specimens were of gem quality, but others had defects such as carbon inclusions, cracks, and crystal twinning. After the initial examinations had been made, more attention could be directed to examining the nature of the photovoltage.

Optical Absorption

To investigate the photovoltaic properties at the surface of a diamond, it is necessary to first establish information about several related problems. It is well known that characteristics of both optical absorption and photoconductivity are found in the spectral response of the photovoltage. In addition, the photovoltage which occurs at potential barriers and inhomogenieties in the bulk of a specimen must be isolated. When these obstacles have been overcome then the surface photovoltage can be investigated as to its spectral response, dependence on light intensity, and surface defects.

The optical transmission of the seventy-four diamonds used in this study was recorded from 1850 Angstroms in the ultraviolet to 16 microns in the infrared. The transmisssion of one large Type IIb diamond (DS-5) was observed out to 40 microns. The optical transmissions at temperatures as low as 77°K were recorded for several Type IIb diamonds (DS-2, DS-5).

The optical measurements of the present investigation were made on two spectrometers whose wavelength ranges overlap. The Beckman

DK-1 is a quartz prism, double beam spectrometer with a spectral range from 1850 Angstroms to 3.5 microns. Its optical path is shown in Fig. 9. The 480 cps light chopper produces an ac output from the light detector. The ac signal is then passed through a band pass filter to increase the signal to noise ratio. The 15 cps light chopper reflects the light beam alternately in the sample and the reference cell providing a frequent zero comparison with the reference cell. The DK-1 uses a lead sulfide detector for wavelengths longer than 450 mμ and a phototube for wavelengths shorter than 600 mμ. This instrument uses a hydrogen lamp for the ultraviolet light source and a tungsten lamp for the visible and infrared light source.

A low temperature cell was constructed to use with the Beckman DK-1 and is shown in Fig. 10. Quartz windows were used which transmit throughout the wavelength range of the DK-1. A dynamic vacuum lower than 10^{-4} torr was maintained in the cell during measurements. The temperature was reduced by filling the dewar with liquid nitrogen, and the temperature was monitored with an iron-constantan thermocouple. Diamond is known to have a high heat conductivity. Thus the temperature of the brass block against which the diamond was pressed was assumed to be a reasonable value for the diamond's temperature. The iron-constantan thermocouple was embedded in the brass block with Saueresin heat conducting ceramic cement.

The Beckman IR-7 was used for the infrared optical transmission studies. It is equipped with two optical interchanges which allow measurements to be made from 2.5 microns out to 40 microns. Its optical path is shown in Fig. 11. Each interchange in the IR-7 is

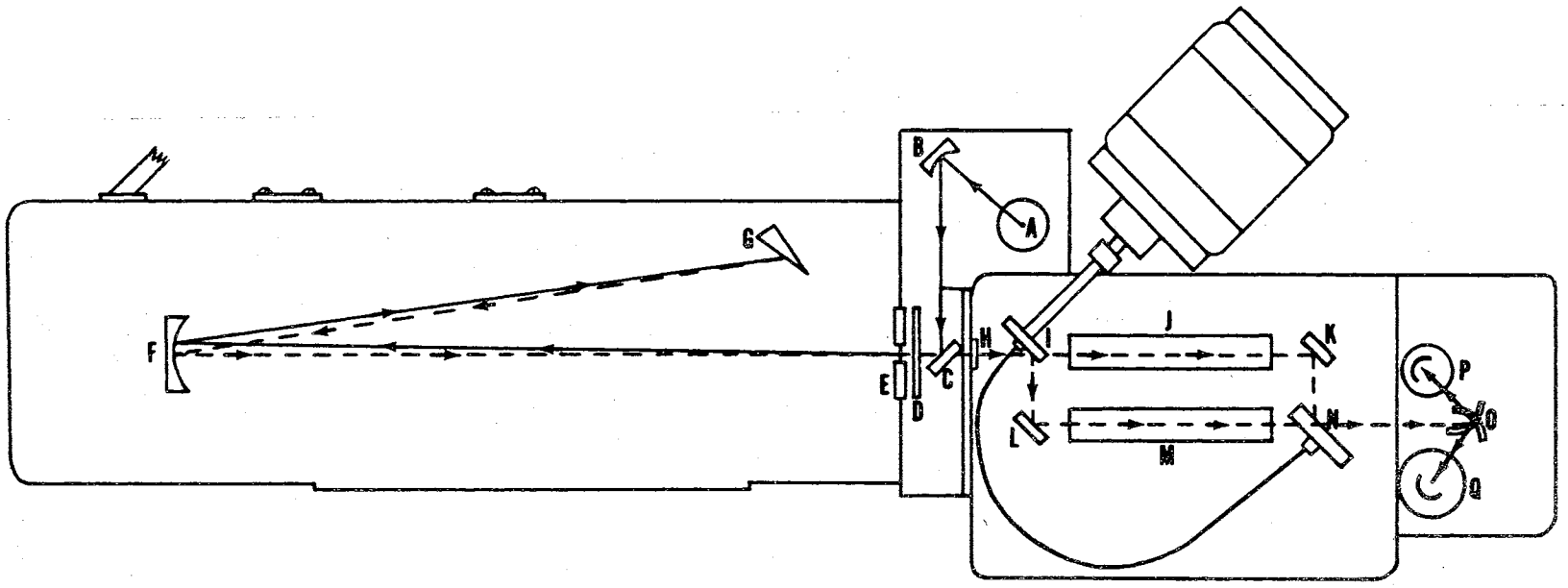

Light from the source (A) is focused on the slit (E) by the condensing mirror (B). The directed beam from the condensing mirror (B) is deflected through the chopper (D) and upon the entrance slit (E) by the slit entrance mirror (C). Light focused on the slit (E) falls on the collimating mirror (F) and is rendered parallel and reflected to the quartz prism (G). The back surface of the prism is aluminized so that light is reflected back through the prism. The desired wavelength of light is selected by rotating the Wavelength Selector which adjusts the angular position of the prism. The spectrum is directed back to the collimating mirror (F) which focuses the selected wavelength on the exit slit (E). Light leaving the monochromator is focused by the lens (H) into the sample compartment, where the beam is alternately switched between the reference path (J) and the sample path (M) by rotating mirrors (I and N) and stationary mirrors (L and K). The beam entering the photocell compartment is focused by the spherical condensing mirror (O) on either the lead sulfide detector (P) or the photomultiplier detector (Q).

Fig. 9. The optical path of the Beckman DK-1.

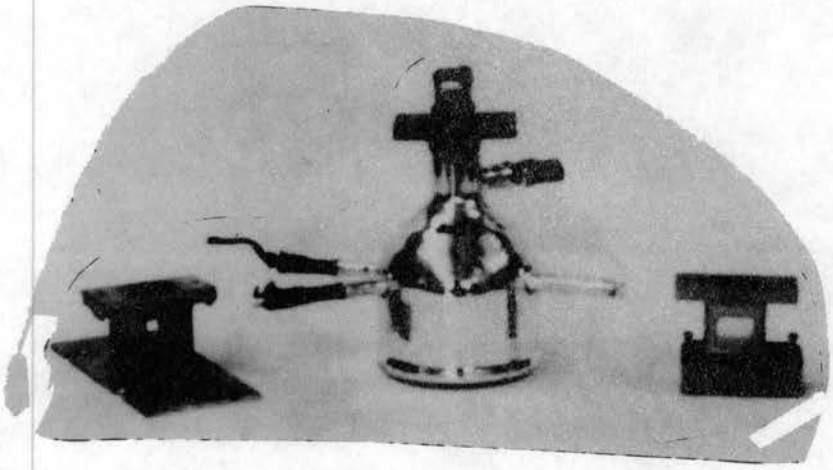

Fig. 10. A low temperature cell constructed for use with the Beckman DK-1 and IR-7. This cell could be used for both optical absorption and photoconductivity measurements.

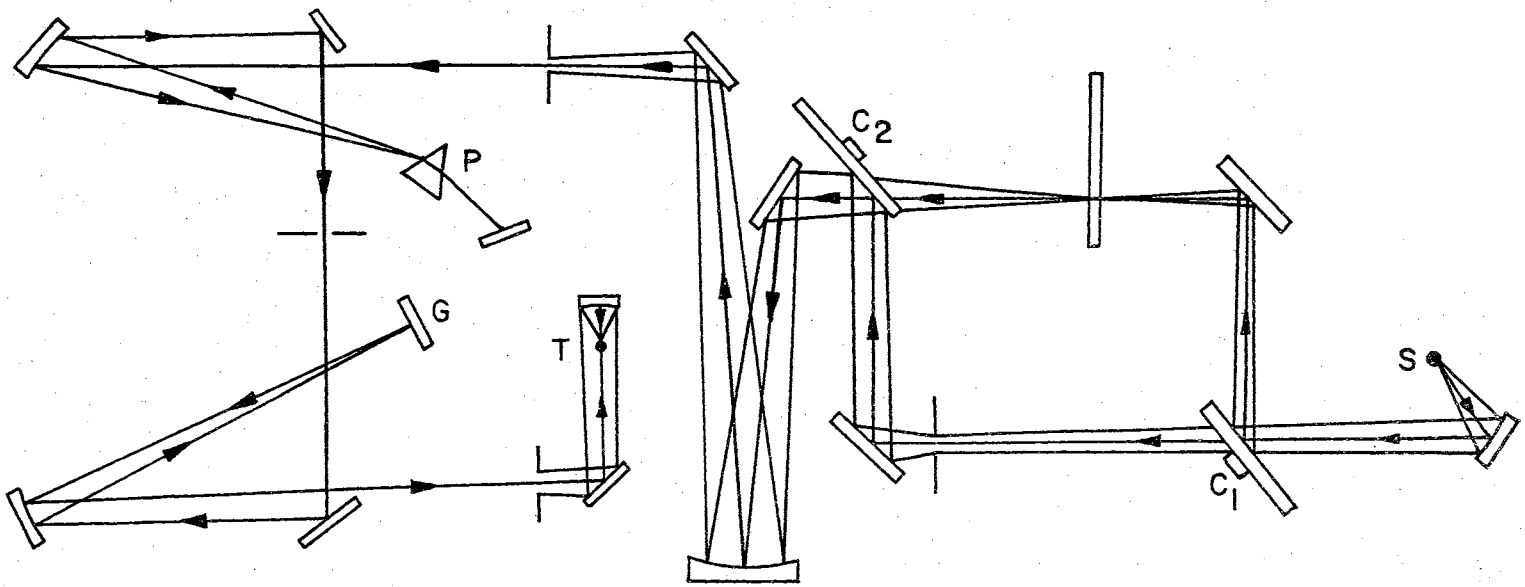

Fig. 11. The optical path of the Beckman IR-7.

comprised of two monochromators. The first monochromator is called an order separater and allows only a narrow band of wavelengths to arrive at the grating, G, of the second monochromator. This technique greatly reduces the problems of the higher order spectrums overlapping and yields the large dispersion available in a grating. The Beckman IR-7 is also a double beam spectrometer with an 11 cps chopper, C, that alternates the light beam in the sample and reference path. It uses a Nernst glower for a light source, S, and a Reeder vacuum thermocouple, T, as a detector. The IR-7 has a resolving power of approximately 0.1 cm^{-1}. One of the accessories with this instrument is a beam condenser that reduces the diameter of the light beam to 1/8 inch. A low temperature cell was constructed to situate the cooled diamond in the concentrated beam. Only the base of this cell needed to be constructed since the dewar and sample holder designed for the Beckman DK-1 sample cell was also intended for use with the IR-7. Fig. 12 shows the IR-7 sample cell and the beam condenser.

Figures 13, 14, and 15 display several examples of the optical transmissions of the diamonds used in this study. From these optical transmissions the diamonds can be assigned a Type. Type I diamonds exhibit 8 micron absorption and have an ultraviolet cutoff above 3000 Angstroms. Type IIa diamonds do not have an absorption band at 8 microns and transmit to wavelengths of 2300 Angstroms or lower. Type IIb diamonds have the optical properties of Type IIa diamonds but have an additional absorption band near 3.5 microns. Table 2 lists some of the observed bands. The fine structure at the activation energy in Type IIb diamonds is resolved at low temperatures as shown in Fig. 13.

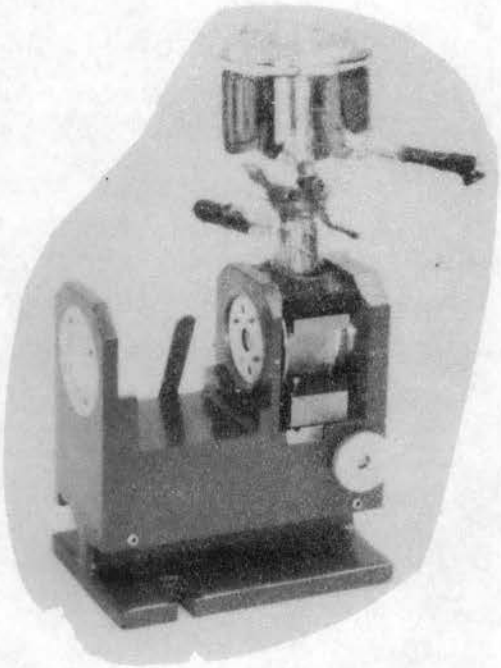

Fig. 12. The sample cell and beam condensor for the Beckman IR-7.

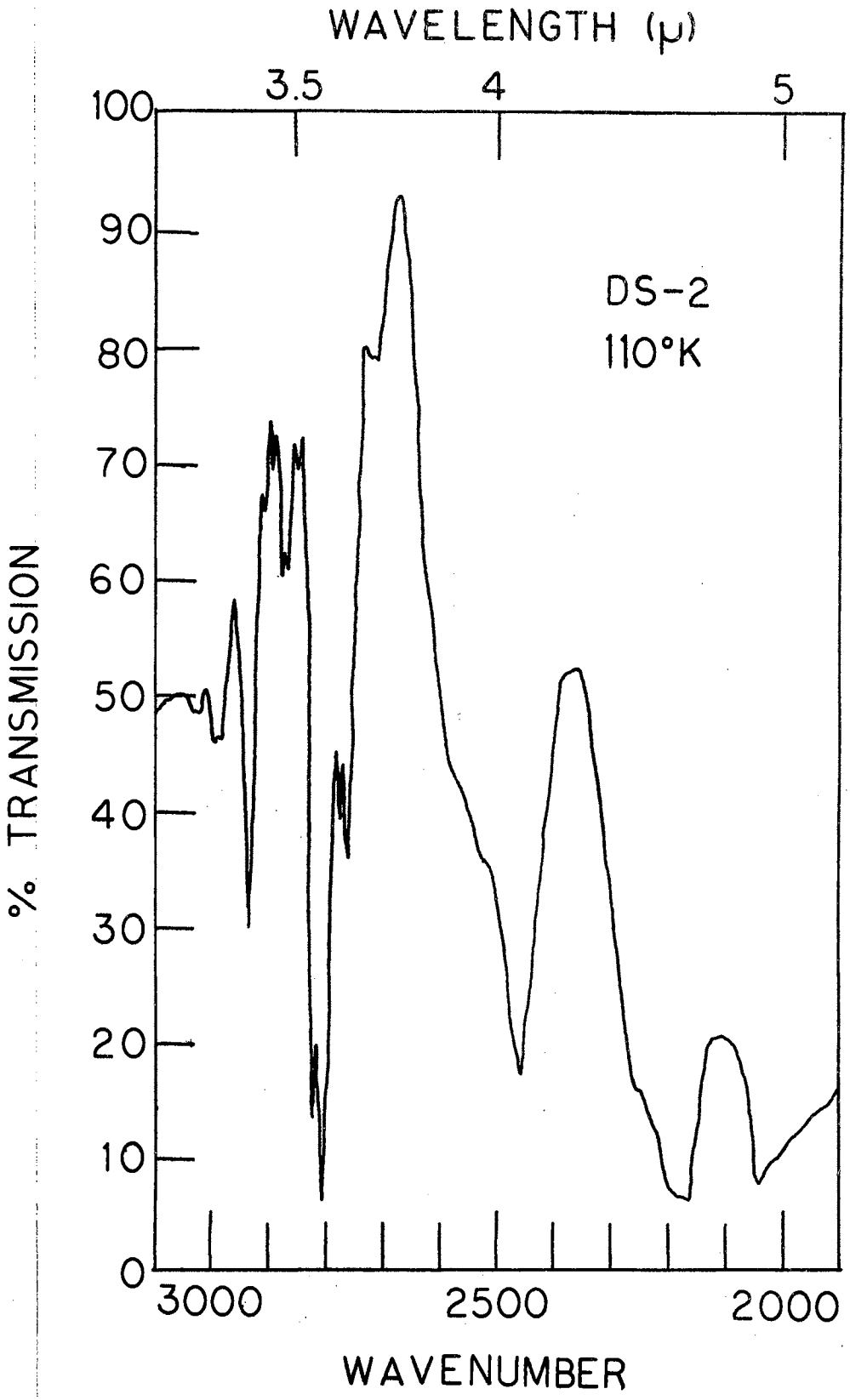

Fig. 13. The low temperature infrared absorption characteristic of Type IIb diamonds.

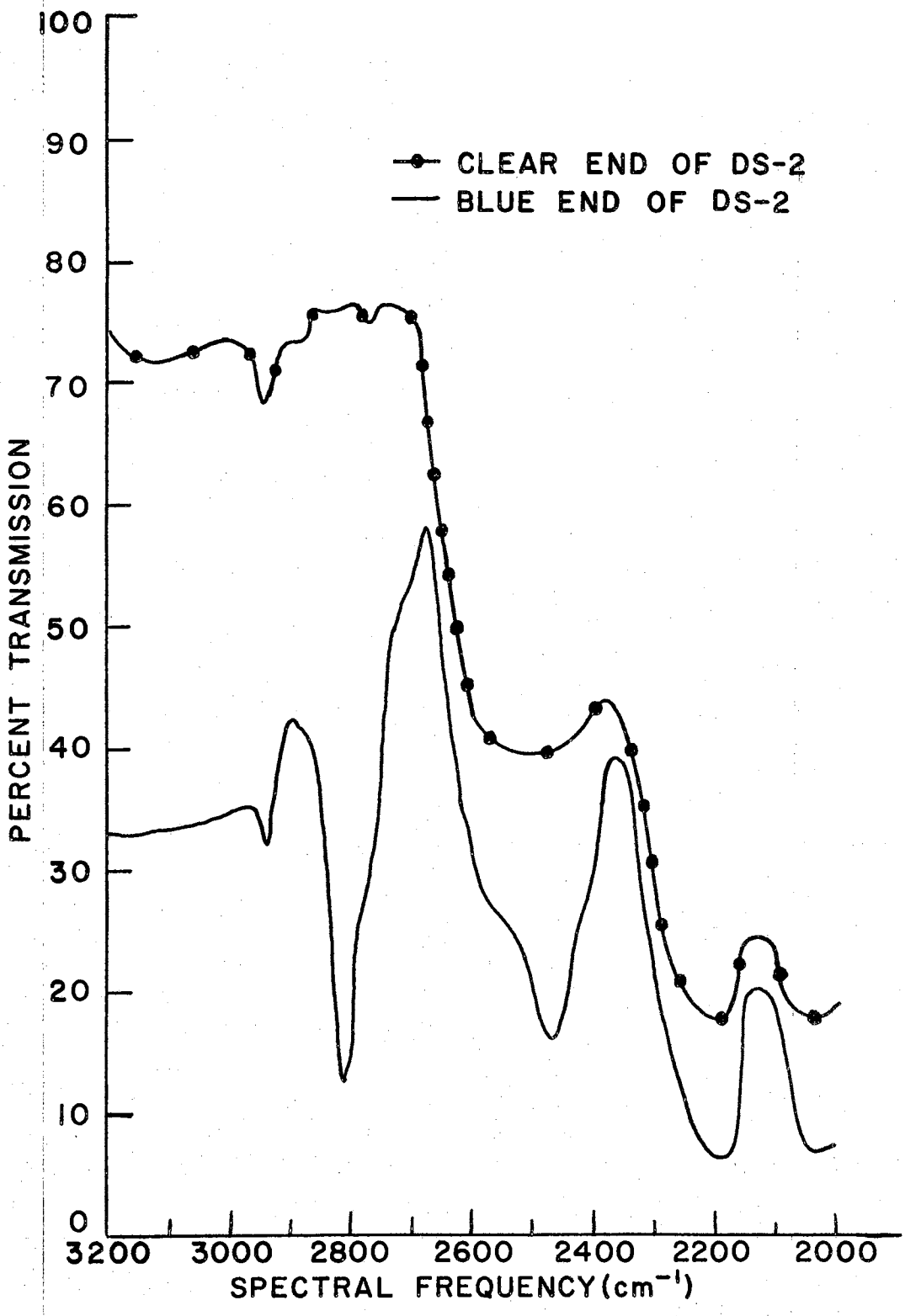

Fig. 14. The infrared absorption in two regions of a Type IIb diamond.

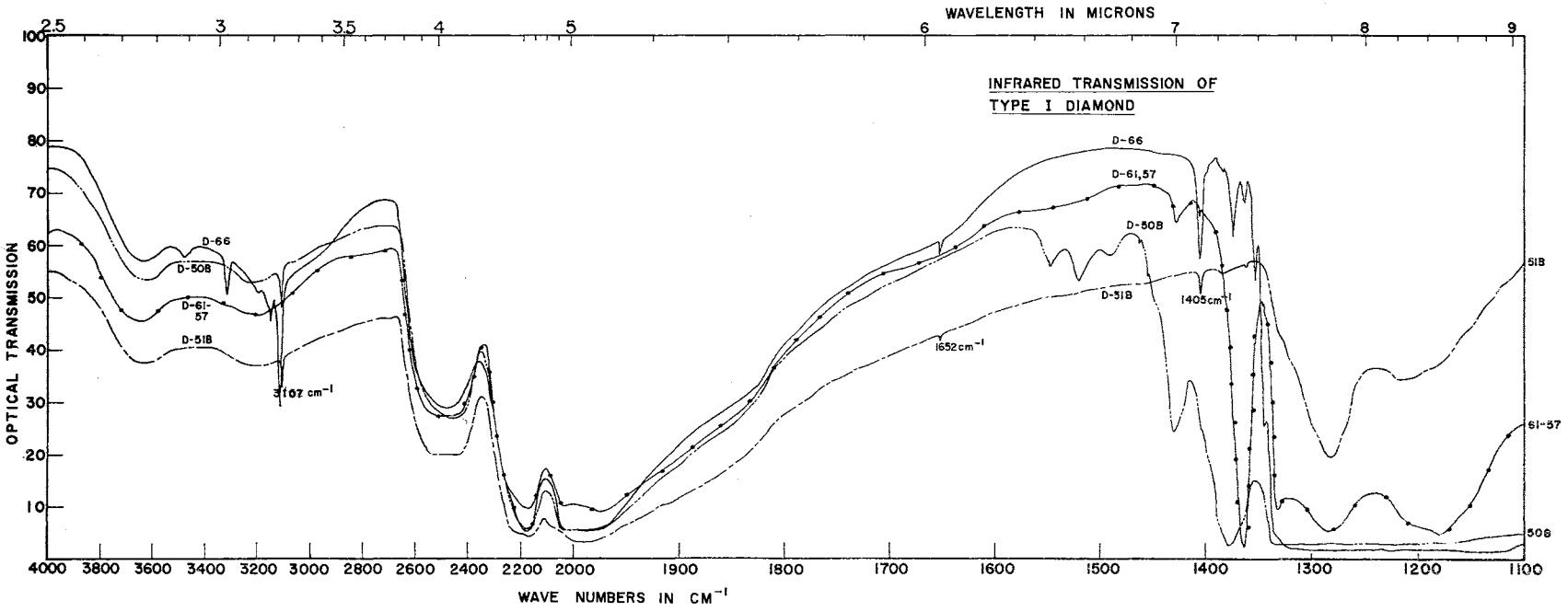

Fig. 15. The infrared absorption of five Type I diamonds.

These values confirm those of Charette (7,8). The optical absorption in two regions of a diamond shown in Fig. 14 exhibits the inhomogeneity found in DS-2. This inhomogeneity is not uncommon in diamonds and presents a great difficulty in many of the investigations on diamond. Type I diamonds display the greatest variety of absorption bands, but all Type I diamonds have the 8 μ absorption in common. Many diamonds are found to be intermediate between the three types of classification.

Photoconductivity

Obtaining the necessary information about the photoconductivity in Type IIb diamonds presented more of a problem. Although some work had been done in this area, it was insufficient for the temperature ranges to be covered in this study, and the resolution of these earlier measurements had to be improved.

The photoconductivity measurements were made using the Beckman DK-1 as a monochromator and substituting the diamond for the detector in the DK-1's recording system. A diagram of this electrical modification is shown in Fig. 16. The photoconductivity was measured with 480 cps chopped light. In the subsequent discussion, the reference to ac photoconductivity will mean the alternating photoconductivity due to the interrupted light beam. The ac photoconductivity had the advantage of being able to use a band pass filter to increase the signal to noise ratio. The sample cell used in the optical absorption measurements was designed to also be used in the photoconductivity experiments.

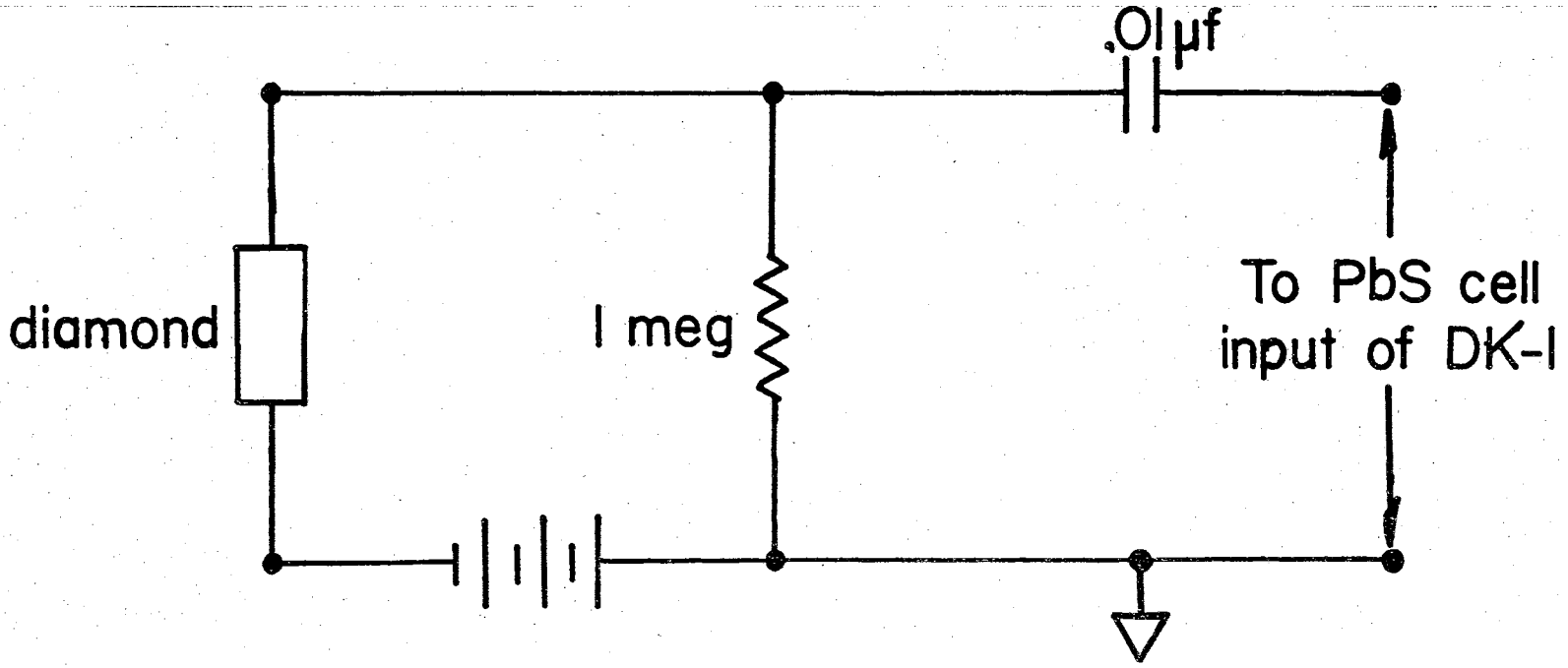

Fig. 16. Electrical modification of the Beckman DK-1 spectrometer recording system.

In the initial investigations while examining the diamond mounted in the photoconductivity cell, the light beam which had passed through the diamond was reflected back onto the diamond. The photoconductivity signal was observed to double. A factor of ten or more was obtained in the signal to noise ratio by using this effect in a multiple path technique for the optical beam. It was realized that since diamond absorbs only a few percent of the light in the region from 3.5 μ to 0.4 μ, the light could be reflected back into the specimen many times by using a cylindrical reflector, thus enhancing the possibility of absorption. Figure 17 shows the cylindrical reflector. The greatly increased signal allowed much smaller slit widths to be used with the monochromator and thus increased the resolution.

As the temperature was lowered, the room temperature photoconductivity peak at 0.7 μ was observed to decrease in magnitude, and at lower temperatures, a great deal of fine structure was noted out to 3.5 μ, the optical limit of the monochromator. This structure is shown in Fig. 18. In a subsequent investigation by Krumme of this laboratory, the photoconductivity in diamond has been examined down to 4°K and out to 16 microns with the conclusions noted in Chapter I.

Photovoltage

With these associated measurements recorded, the photovoltage at the diamond surface was examined. A Beckman DU was used as a monochromator, and its optical path is essentially the same as the DK-1 without the light chopper. The DU has a larger prism and is optically more

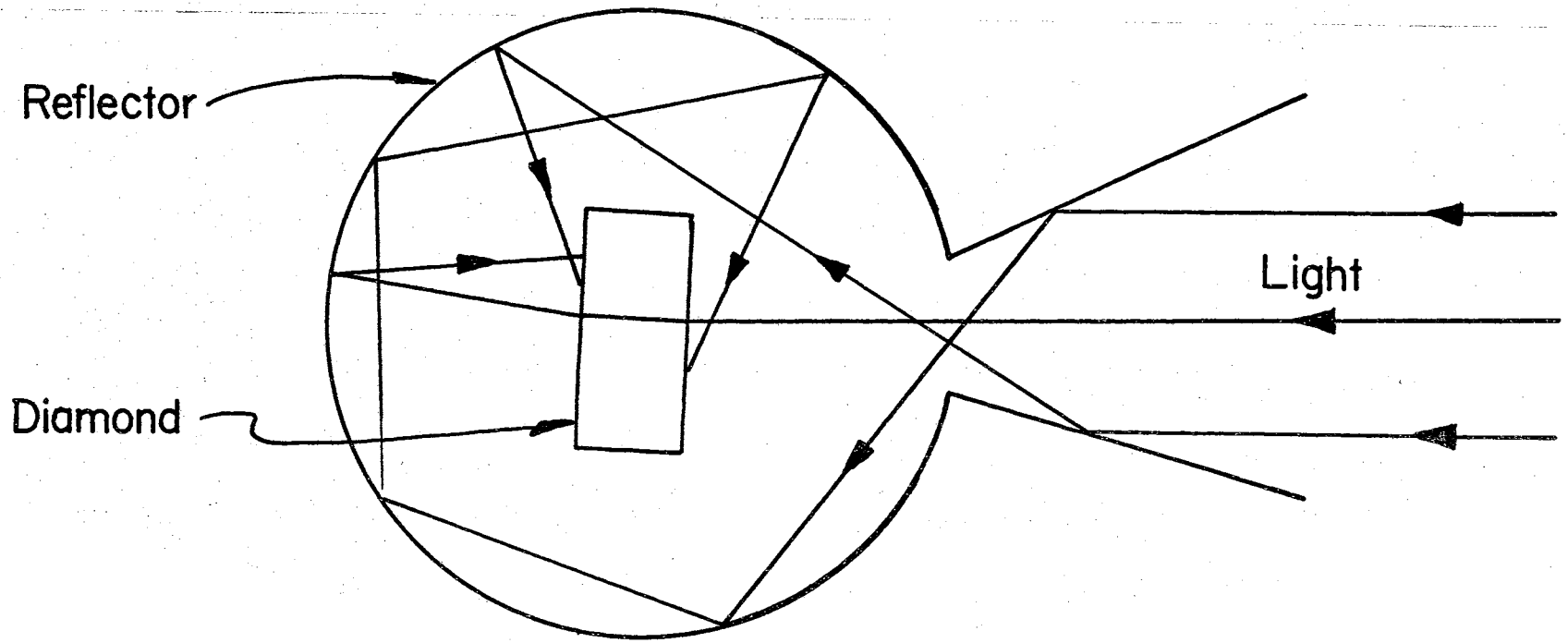

Fig. 17. Cylindrical reflector used to enhance absorption for the photoconductivity.

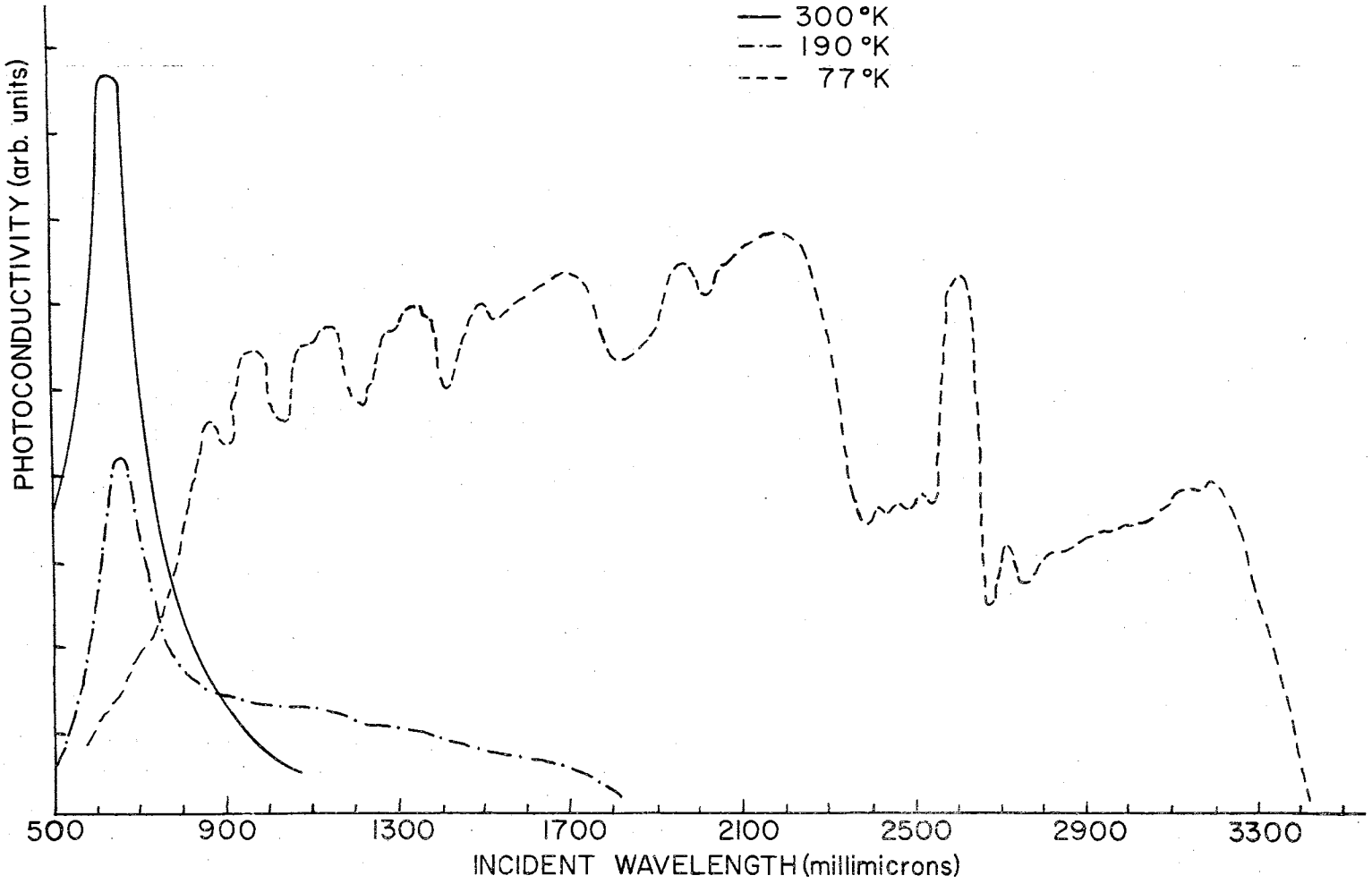

Fig. 18. The spectral response of the photoconductivity for Type IIb diamond at three temperatures.

powerful than the DK-1. The energy distributions of the monochromators used in the present investigation were obtained with a Gaertner compensated thermopile and a Leeds and Northrup galvanometer for the wavelength range from 3.5 μ to 0.325 μ. These measurements were repeated to give an r.m.s. deviation of less than 5 percent. The number of photons per unit time, N_p, in the light beam for a given slit width of the monochromator is obtained in the following manner. The energy of one photon E_p is given by $E_p = h\nu$ where h is Plank's constant and ν is the frequency of the photon. If E_T is the energy flux striking the thermopile and assuming no loss on the thermopile window and total absorption of the thermopile,

$$N_p = E_T/E_p = E_T/h\nu = E_T.\lambda/hc = K(E_T.\lambda)$$

or $$N_p \propto E_T.\lambda$$

where c is the speed of light, K is $1/hc$, and λ is the wavelength of the incident light. Thus the relative photovoltage per photon per sec., V_p, is $V_p = V_m/E_T.\lambda$ where V_m is the measured photovoltage.

The relative number of photons per sec in the monochromator's light beam for the wavelength range 2000 to 7000 Angstroms was measured using an RCA 1P28 photomultiplier tube, a Hamner N-401 high voltage supply, and a Hewlett Packard 410-B Vacuum tube voltmeter. The electrical schematic for these instruments is shown in Fig. 19. The photomultiplier tube is a photon counter, that is, the output current of the photomultiplier, I_p, is proportional to the photon flux rate, N_p. However, in order to obtain the photon flux for various wavelengths, the output of the photomultiplier must be compensated for the

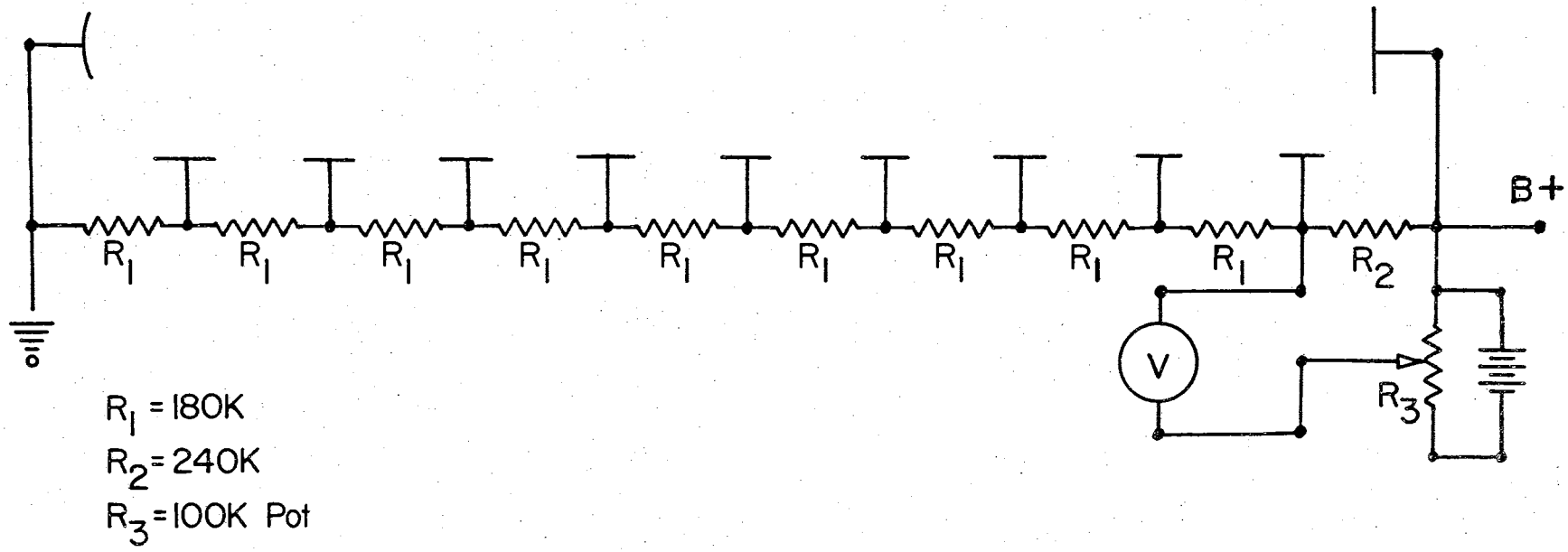

Fig. 19. The electrical schematic of the RCA 1P28 photomultiplier tube used in calibrating the spectral output of the spectrometers.

spectral sensitivity of its cathode and absorption in the photomultiplier window. The spectral sensitivity curve published by the manufacturer was used in these calculations. The electrical measurements from the photomultiplier tubes are repeatable to less than one percent. However, in a private communication with the National Bureau of Standards, it was learned of their recent concern over the calibration standards in the ultraviolet wavelengths. From the comments of the N.B.S., the manufacturer's spectral sensitivity curve is estimated to be reliable to approximately ten percent. By illuminating as much of the photomultiplier cathode as possible to minimize local variations, and by comparing the responses of several tubes, this figure of merit is felt to be a reasonable value.

The photomultiplier tube's spectral sensitivity, S, is defined as the fraction of incident photons that will be counted by the photomultiplier. Therefore, the number of photons per sec, N_p, is

$$N_p = P/S = K'(I_p/S)$$

where P is the number of photons per sec counted by the photomultiplier, $K' \equiv P/I_p$, and I_p is the photo current of the photomultiplier tube.

The relative photovoltage per photon per sec, V_p, is obtained from

$$V_p = V_m \cdot S/I_p .$$

A Cary Vibrating Reed Electrometer was used to detect the photovoltage. Various input resistors can be used with this instrument, and all measurements that required the maximum photovoltage signal were made with a 10^{12} ohm input resistor. With this input resistance the Cary Vibrating Reed Electrometer is capable of detecting a current of

10^{-17} amps. This represents about 64 electrons per second.

A low temperature photovoltaic cell was constructed to use with the Cary Vibrating Reed Electrometer. This cell is shown in Fig. 20 and 21. The sample is easily mounted with the cell disassembled, and then the seal is soldered with Wood's metal. The temperature of the diamond was monitored with an iron-constantan thermocouple embedded in the brass block on which the diamond was mounted. The diamond was cooled by either blowing pre-cooled nitrogen into the dewar or by pouring liquid nitrogen directly into the dewar. The sample cell could be used with a dynamic vacuum, or by closing the Hoke valve in the vacuum line it could be used with a static vacuum. It was found that the vibration from the vacuum system did not introduce any detectable noise into the system, and therefore, all measurements were made with a dynamic vacuum. This has the advantage that the vacuum can be continually monitored and maintained for long periods of time.

A portable vacuum system was constructed using a Welch Duo-Seal 1402 B roughing pump and a glass oil diffusion pump that was built in our glass shop. Two large stopcocks allowed a minimum inside bore of 15 mm and thus insured a greater rate of evacuation. The entire vacuum system was constructed of the large bore glass tubing except for a rubber vacuum hose between the diffusion pump exhaust and roughing pump. The rubber hose permitted the roughing pump to be lowered to the floor and therefore reduced mechanical vibrations in the vacuum system. The vacuum system is shown in Fig. 22. The vacuum was monitored with a Vacuum-Electronics Corportion non-burnout ionization

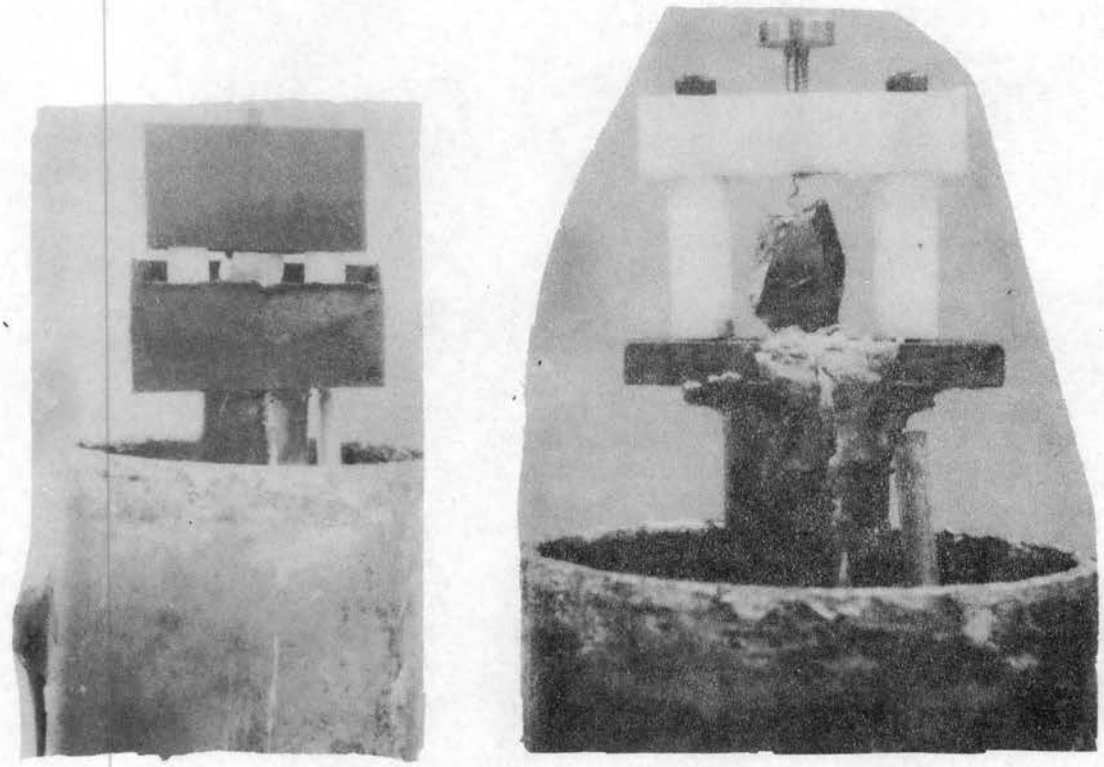

Fig. 20. In the photovoltaic cell shown above, diamond DS-5 is soldered to the brass base of the dewar seal. The sample is then masked so that only the grid contact is exposed to light.

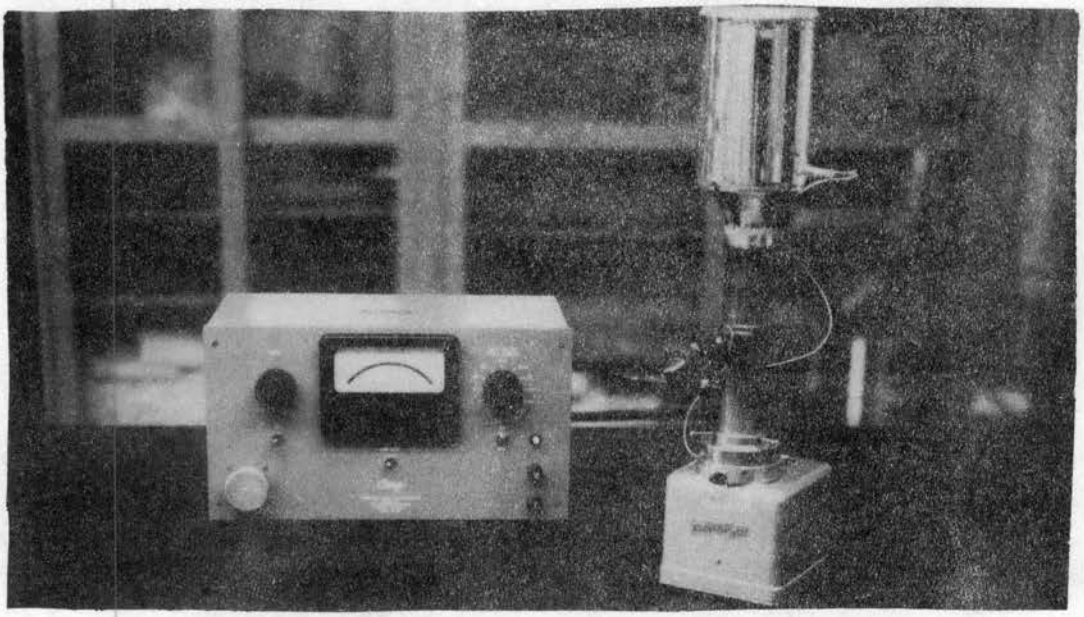

Fig. 21a. The assembled low temperature photovoltage cell is shown attached to the Cary vibrating reed electrometer.

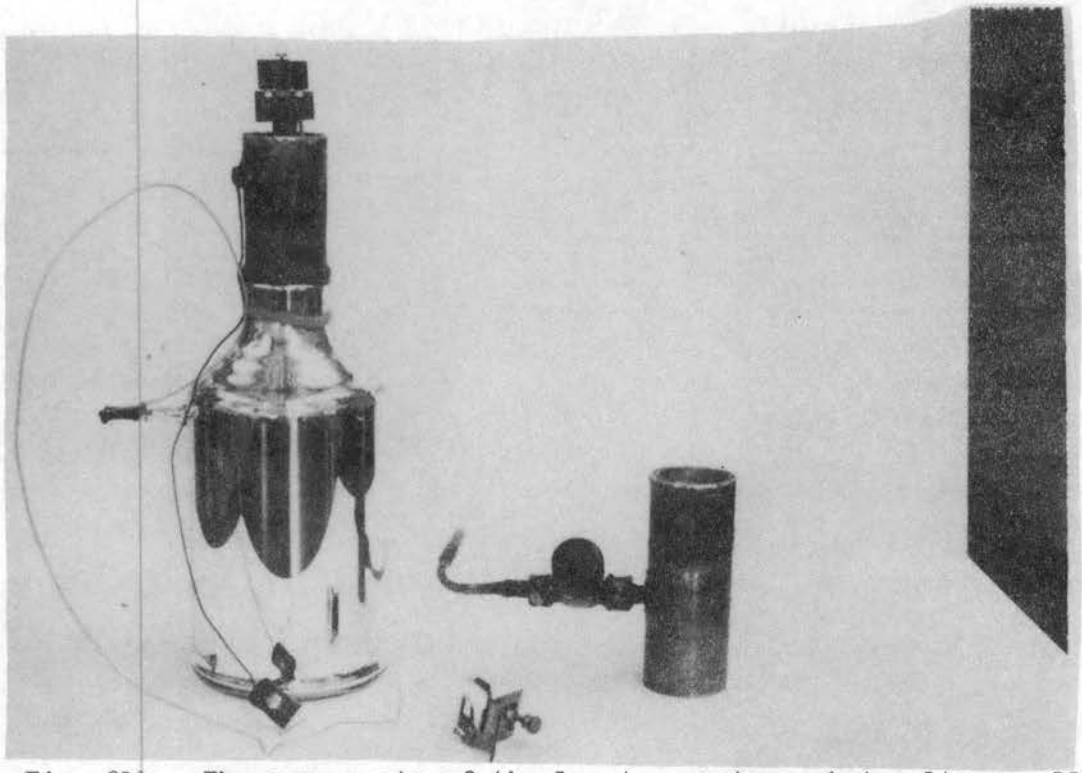

Fig. 21b. The components of the low temperature photovoltage cell.

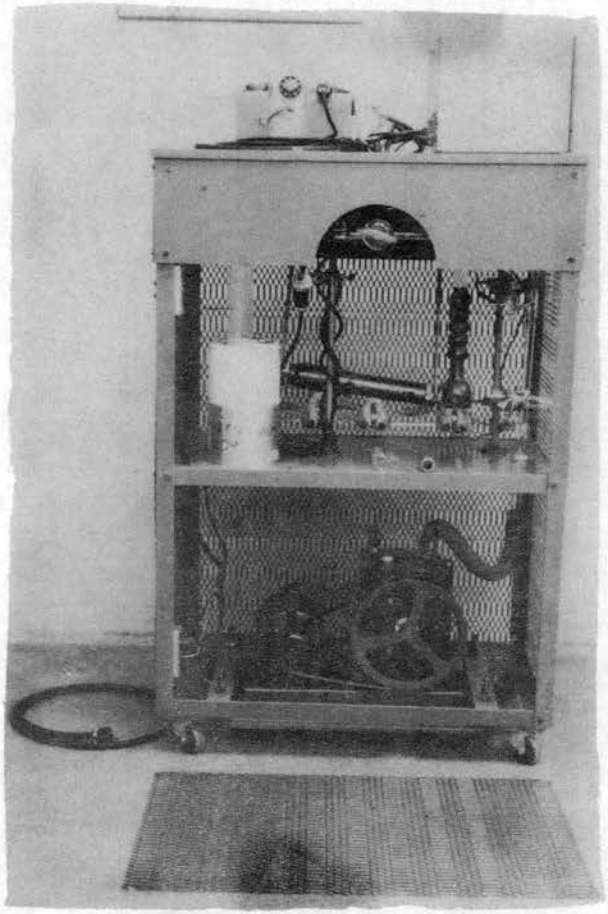

Fig. 22a. The portable vacuum system.

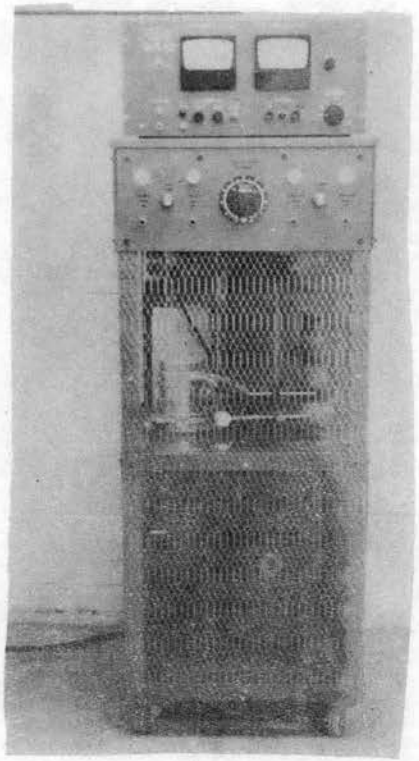

Fig. 22b. The vacuum system control panel.

gauge and two thermocouple gauges. One thermocouple gauge was located at the intake of the diffusion pump and the other at the sample cell joint. The ionization gauge was also located at the sample cell joint. This vacuum system was found to reach a vacuum of 5×10^{-9} torr in two weeks of pumping with frequent heating of the glass tubing to 450°C and cooling of the cold trap with liquid nitrogen. An Edward's High Vacuum regulated leak mounted near the ionization gauge was used for calibrating the gauges. Most photovoltaic measurements were made with a vacuum of 5×10^{-6} torr since this level could be quickly reached and maintained.

The photovoltage was observed by flashing a beam of light from the monochromator into the diamond. The input capacitance of the sample cell and electrometer, and the high input resistance of the electrometer produced an RC time constant which restricted the response time to approximately one second. Thus, the photovoltage would peak in several seconds and slowly return to zero in one or more minutes as shown in Fig. 23.

If the diamond is activated with wavelengths shorter than 1250 mμ and not allowed to relax, substituting light with a wavelength longer than 1250mμ produces a photovoltage polarity opposite that obtained with the same wavelength of light on the relaxed crystal. The difficulty of making repeatable photovoltaic measurements has been noted by earlier experimenters. It was found that the photovoltage could be repeated to within several percent of the original measurement if fifteen minutes elapsed between successive readings. Therefore, this degree of activation of the diamond was

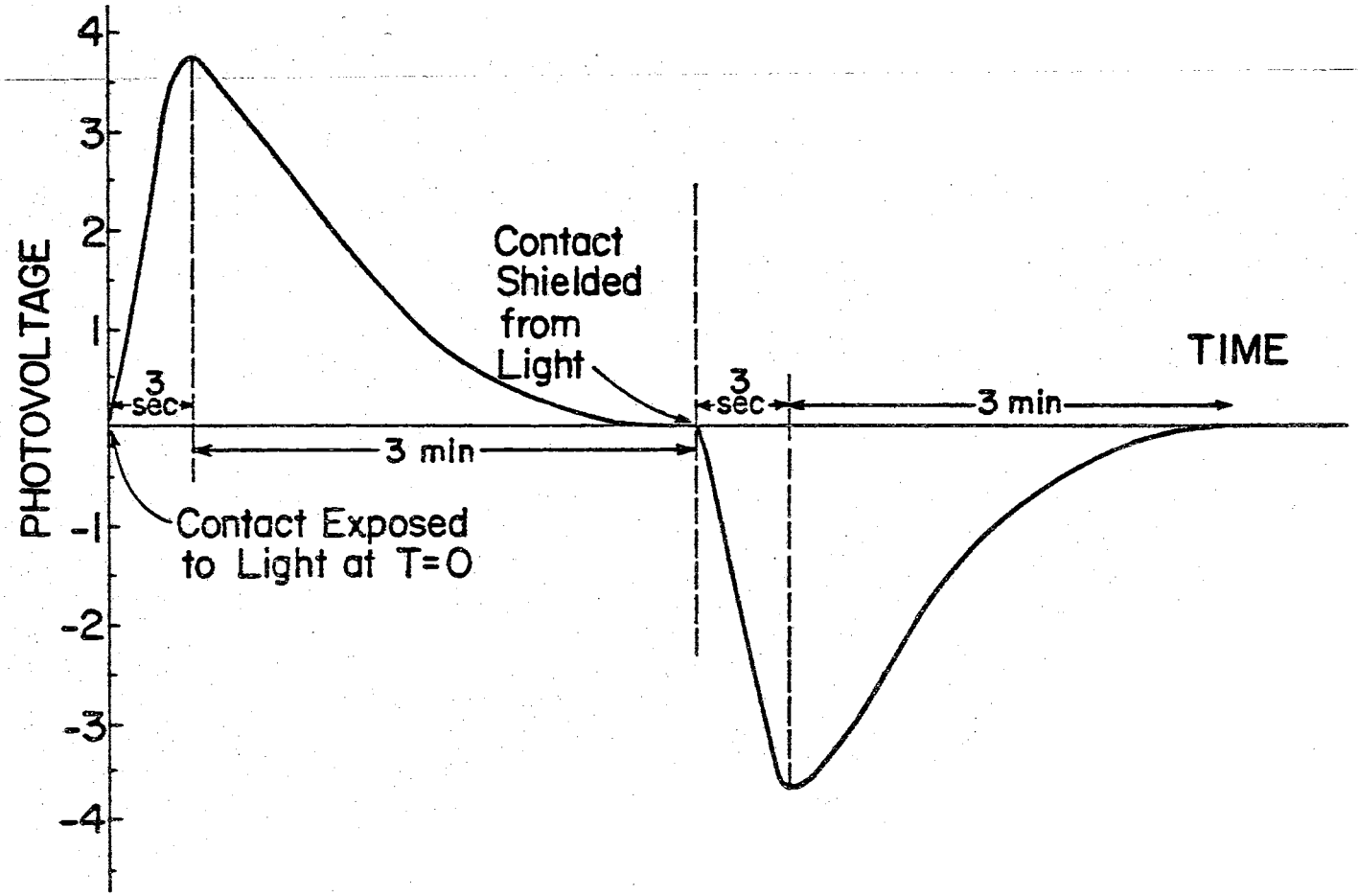

Fig. 23. The time dependence of the photovoltage.

tolerated, and most measurements were made point by point with a fifteen minute interval between successive recordings.

The photovoltage at a diamond to tungsten probe contact was examined for seventy-four diamonds. This diamond collection includes twenty-five Type I, ten Type IIa, five Type IIb diamonds. Thirty-four diamonds had properties intermediate between the three major classifications. This general survey confirmed Robertson, Fox, and Martin's observation that Type II diamonds in general show a much stronger photovoltage than Type I. However, a few diamonds that had optical properties intermediate between the types displayed a strong photovoltage. Examples of this are D-10, D-46. If a light shines on a diamond to metal contact, the maximum photovoltage observed by the Cary Vibrating Reed Electrometer for Type I diamonds is of the order of 4 millivolts while for Type IIa and Type II b diamonds it is of the order of 200 millivolts. However it should be noted that diamonds which were good photoconductors had higher observed photovoltages. The results of these measurements are shown in Table 2. More will be said of this correlation in Chapter IV.

The diamonds were also examined to correlate their strength and color of luminescence with the photovoltage. No direct correlation was observed and as opposed to Robertson, Fox, and Martin's (1) experience, several diamonds which luminesced brilliantly showed only a small photovoltage while other diamonds which luminesced only moderately or even weakly displayed strong photovoltages.

As shown in Fig. 24 when two similar metal contacts are made to

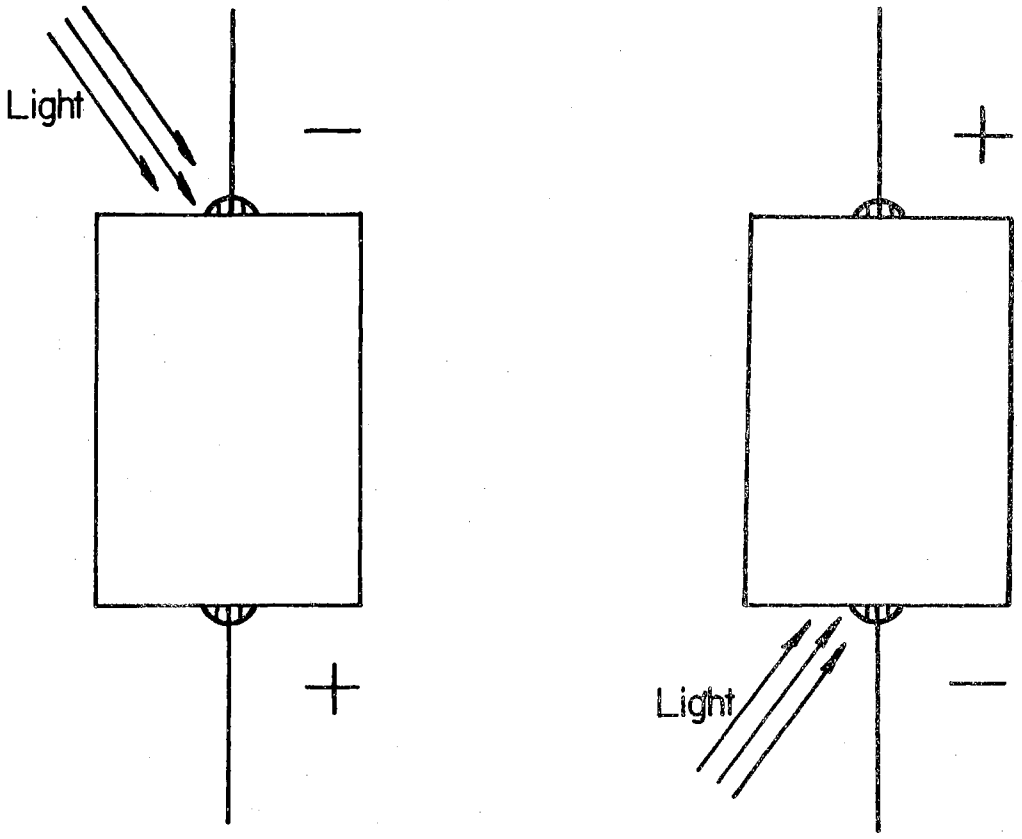

Fig. 24. Illumination of the contacts at the contact of a metal and homogeneous semiconductor.

a homogeneous semiconductor and only one contact is exposed to light, the polarity of the photovoltage should reverse itself when the other contact is then exposed to the light. Thus at the illuminated contact, the homogeneous semiconductor always maintains the same polarity with respect to the metal. However, if the semiconductor is not homogeneous, this will not always occur.

The experimental advantages of having a diamond with a low internal resistance was discussed in Chapter II. Of the diamond Types only Type IIb has a low resistivity. Therefore the Type IIb

diamonds are examined with tungsten probes to obtain a homogeneous specimen for the photovoltaic studies. A survey of the diamond collection produced several specimens which had the desired characteristic. One large specimen (DS-5) was chosen for the bulk of these photovoltaic studies because of its homogeneity, low internal resistance, and large flat surfaces. The polarity of the photovoltage for all of homogeneous diamonds examined made the diamond positive with respect to the metal at the illuminated contact.

Many types of probes were used to detect the photoconductivity and the surface photovoltage in diamond. Figure 25 shows several of the techniques employed. Although various procedures for cleaning the diamond were tried initially, the following sequence was found to be satisfactory. The diamond was agitated for ten minutes in acetone and five minutes in distilled water. Then it was placed in a beaker of aqua regia for 30 minutes and subsequently agitated in distilled water for five minutes. Finally it was agitated in methyl alcohol for five minutes. A refluxer using ethyl alcohol was found to be an excellent degreaser and was used as a final step to give strongly adhering evaporated metal contacts.

The evaporated metal contacts were formed in the following manner. Figure 26 shows the arrangement of the components in the Consolidated Vacuum plating system. Baffle A shielded the diamond from the filaments B and C. After a vacuum of 1×10^{6} torr had been reached, the filaments B and C were heated to drive off absorbed gases, greases, etc. The plating filament C was held at the melting temperature of the metal for only a few seconds and then cooled so

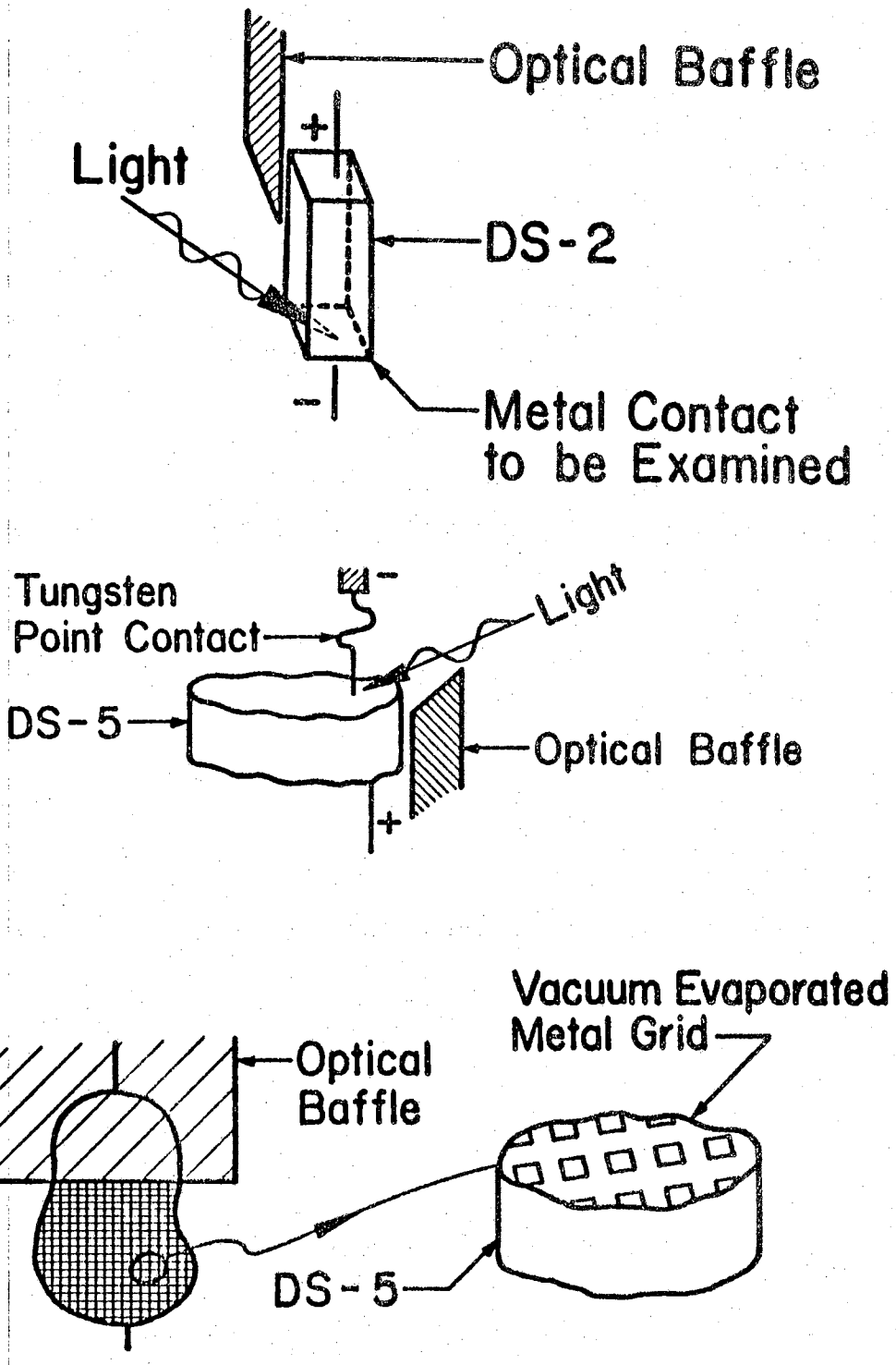

Fig. 25. Three metal to diamond contacts examined in this study.

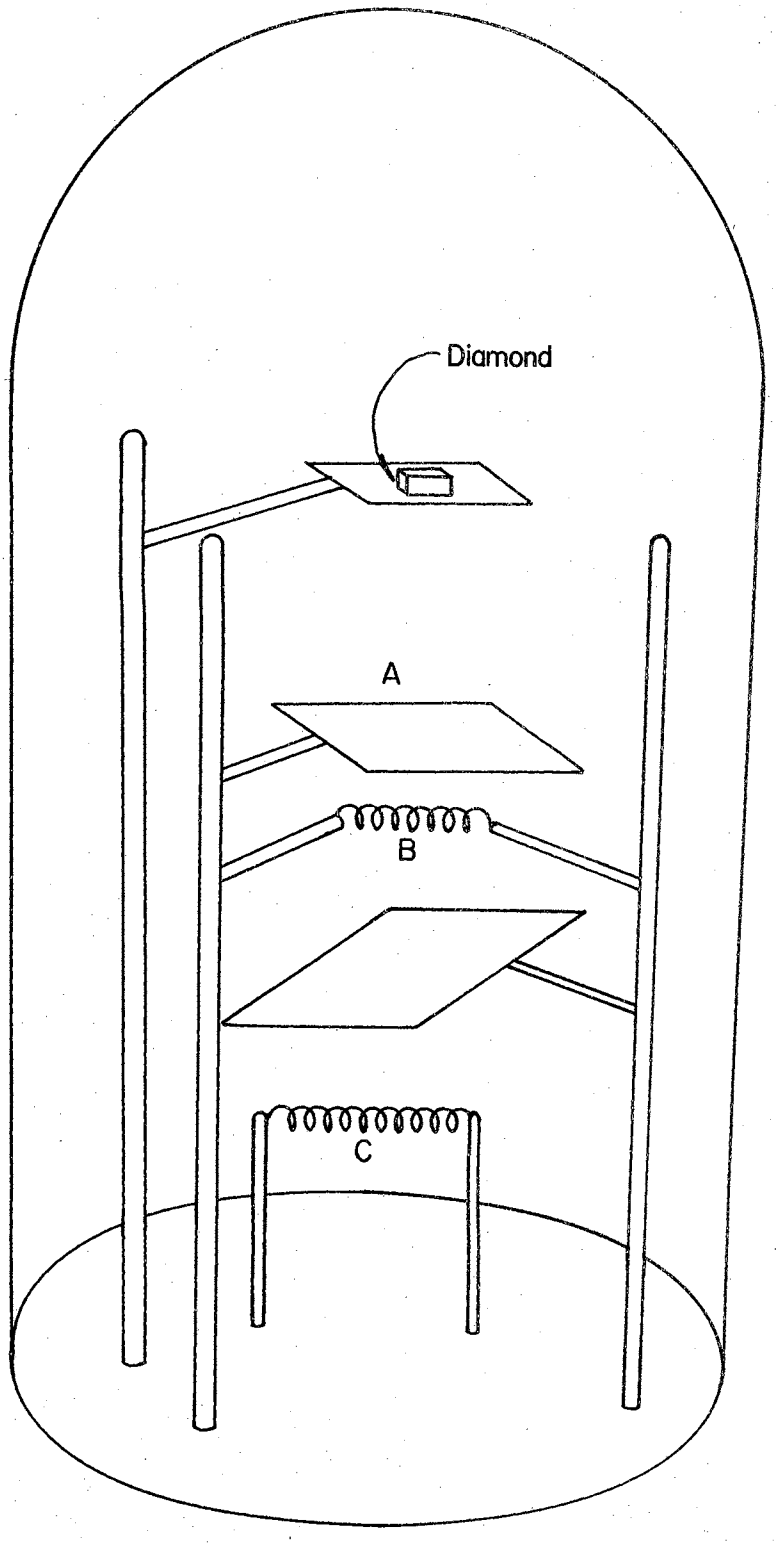

Fig. 26. The vacuum plating system used to produce evaporated metal contacts.

that the metal to be plated would not be exhausted. After the filaments had been cleaned, baffle A was moved aside and the diamond brought into the close proximity of preheating filament B. The temperature of the diamond was allowed to increase to approximately 600°C and maintained for several minutes. The diamond was then brought approximately six inches above plating filament C, and the temperature of this filament was increased to the melting point of the metal to be plated.

The grid pattern was produced by using a lathe to wind 0.0007 inch tungsten wire in 0.0014 inch threads on a brass plate with a half-inch hole in it. The wire was bonded with epoxy on the ends of the plate, and then the wires on one side were cut away. The plate was cleaned in methyl alcohol, and the diamond placed on top of the wires. This plate is shown in Fig. 27. The diamond was placed on the wires, and

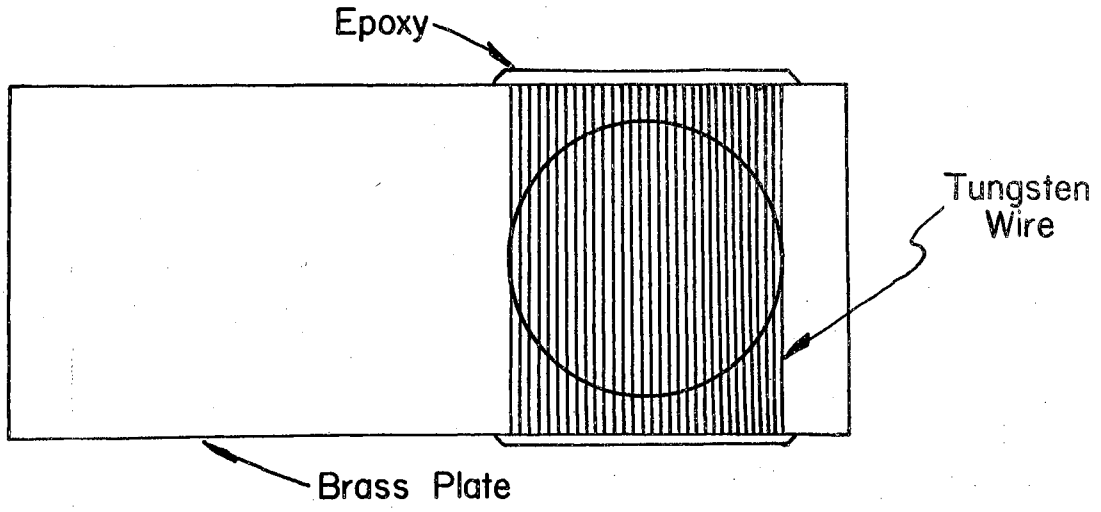

Fig. 27. The stencil used to produce the evaporated metal grid pattern.

the metal was then evaporated on as described above. After the first plating the diamond was turned 90° and replated to give the complete grid. The grid contacts had the advantage that the light could shine directly on the diamond to metal junction.

Metals evaporated on the diamond included aluminum, silver, gold, and platinum. These contacts appeared to adhere well, but were generally rectifying, and the electrical noise levels were comparable ro or greater than those with silver paint. Since silver paint has been the contact to diamond frequently used by earlier investigators, the quality of other contacts will be compared to it.

The tungsten probes were mounted Sylvania tungsten whiskers. They were quite sharp and, therefore, created a high local pressure on the diamond surface. Probes of gold, silver, platinum and copper were also used. These probes were filed to produce the final sharp point. The metallic point probe contacts were found to be highly rectifying. The degree of rectification could be increased by "forming" with a Tessla coil or a current surge from a battery. The highest photovoltages obtained in this study were with metallic pressure probes. The noise level with these probes was equal to or higher than those with silver paint. If the point contact of the probe was painted with Dupont 4817 silver paint and then pressure applied on the probe-to-diamond contact, a relatively low noise contact could be obtained. Generally the paint has to cure for three or four days for the lowest noise levels and for the contact resistance to stabilize, but it can be used after a one hour drying time. The curing of the paint can be hastened in an oven at 80°C. It was ob-

served, however, that contacts cured by heating had a higher noise level than those cured slowly.

Several contacts were made by directly soldering to diamond. Both indium and Wood's metal adhered to diamond if the diamond was heated to the melting point of the metal. Again the noise levels of the contacts with these metals were not an improvement over the Dupont 4817 silver paint.

Viking LS 232 liquid alloy solder composed of thallium and indium dissolved in mercury appeared to wet diamond, but the noise level was very high.

All of the contacts mentioned above were generally rectifying and if a volt-ohmmeter was used to measure the rectification, typical resistance ratios varied from 1:1 to $1:10^4$.

By far the best contacts made to the diamond from an electrical and mechanical point of view are made by the titanium hydride bridge technique. The 325 mesh titanium hydride powder is suspended in a solution of Acryloid resin and amyl acetate. This mixture is applied to the diamond and a special solder alloy, Incusil 15 from Western Gold and Platinum Company, sprinkled onto the dried mixture and caused to stick by a drop of amyl acetate. The diamond is then placed in a vacuum furnace while it is evacuated to approximately 10^{-5} torr. The diamond is then heated to 705°C. for approximately ten minutes. The decomposition of the titanium hydride with the release of atomic hydrogen occurs rapidly near 700°C. Low temperature solder contacts can now be made to the "bridge" of metal on the diamond. The Ti-bridging contact was the least rectifying contact studied. Noise with

this contact was reduced by approximately a factor of 100 over that of silver paint contacts. The contact resistance was also reduced by two orders of magnitude. The contact adheres tenaciously and reportedly breaks in the diamond before it is able to be sheered off. This contact has a number of disadvantages. Although it can be removed with a solution of $\frac{1}{2}$ HNO_3-$\frac{1}{2}$ HF heated to approximately 90°C, it leaves an etched surface. In addition, it requires the diamond to be heated and therefore could conceivably alter the specimens. Since the titanium hydride bridging technique does permently etch the surface of the specimens and a rectifying contact is of greater interest in an examination of the photovoltage, this contact was studied on only one diamond.

It was noted that a point contact to a Type IIb diamond surface usually will not produce a detectable photovoltage at room temperature. However, occasionally a photovoltage as large as 600 mv will be produced when the probe is in a photovoltaically sensitive region. The large signals are as apt to be found on apparently flat surfaces as well as rough edges. Since no correlation of the surface photovoltage with visible surface defects was observed, the possibility of a correlation with surface contaminations was examined. A tungsten probe was positioned on the diamond surface at a location producing no photovoltage. The probe was wetted with such compounds as methanol, acetone, carbon tetrachloride, nitric acid, hydrochloric acid and various oils. No photovoltage was produced by the addition of any of these compounds. When the probe is positioned to a photovoltaically sensitive area, and wetted with the Viking LS 232 liquid alloy solder,

the initial photovoltaic sensitivity disappears. When a contact is made to the photovoltaically sensitive area with the liquid solder alone, no photovoltage occurs. Only when the tungsten probe alone is pressed to the sensitive region is a photovoltage produced. These measurements were made on DS-2 which had the Ti bridge contact as the second electrical contact. The time decay of the photovoltage observed in the other studies did not occur with this arrangement. When the light shone on the diamond to tungsten probe contact, a steady voltage of up to 50 mv was obtained. This behavior will be discussed further in Chapter IV.

The spectral response of the photovoltage has been reported by Bell (34). A reexamination and extension of these earlier measurements has produced a clearer picture of the spectral dependence of the photovoltage. The structure is shown in Fig. 28, 29, and 30. All of the structure in the photovoltage can now be correlated with the optical absorption and photoconductivity.

The "anomalous" peak at 445 mu in the photovoltaic spectrum is believed to be a consequence of instrumental complications. Although this peak appears in the uncorrected photovoltaic spectrum obtained from the tungsten bulb, it is not in any of the data obtained with the hydrogen lamp and disappears from the tungsten bulb data when the bulb's spectral output is introduced into the corrected photovoltaic response. The peak is believed to be due to the increase in the sensitivity of the photovoltage and the decrease in the photon output of the tungsten bulb at lower wavelengths.

The ultraviolet spectral response of the photovoltage shows the

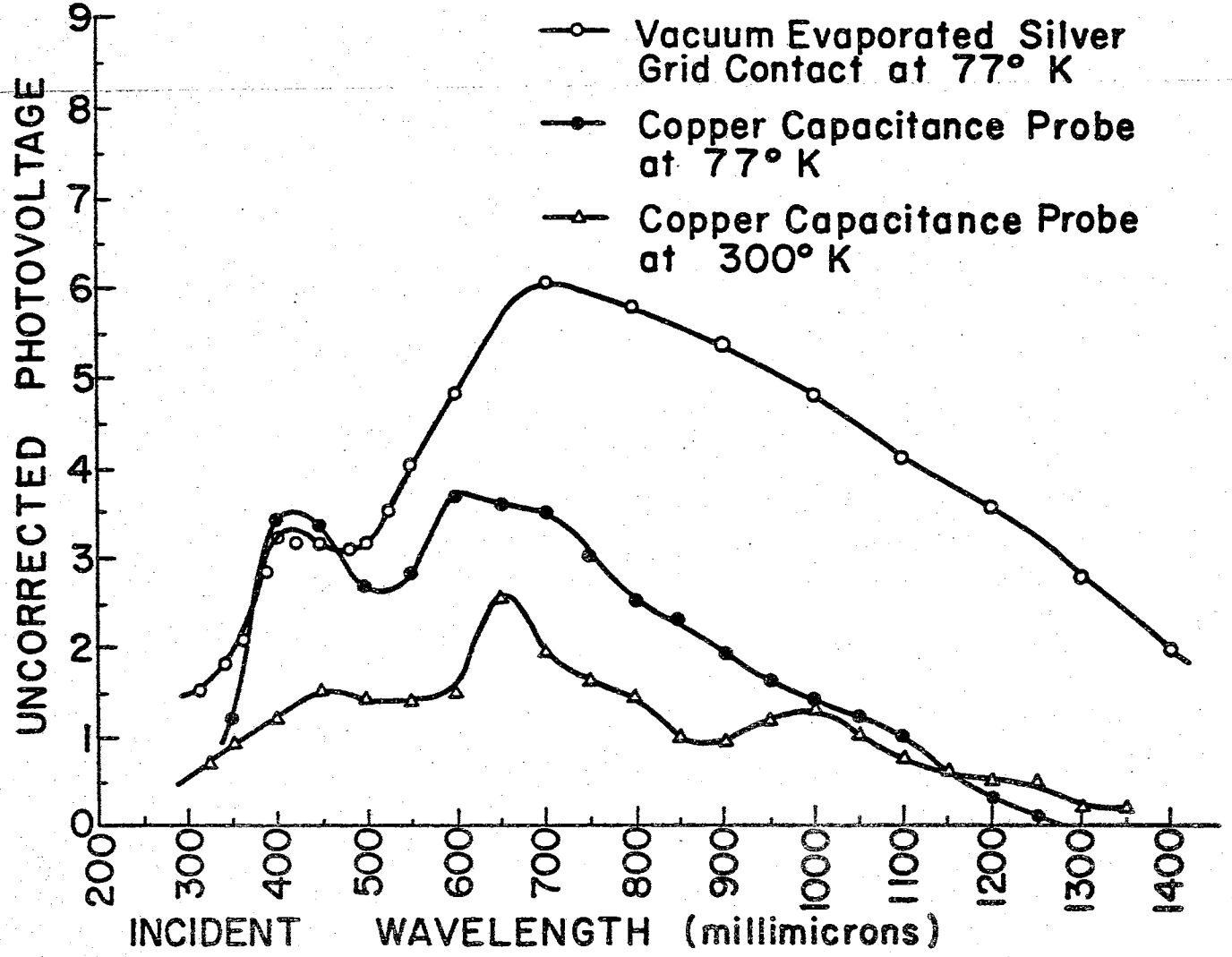

Fig. 28. Experimental photovoltage using a tungsten lamp source.

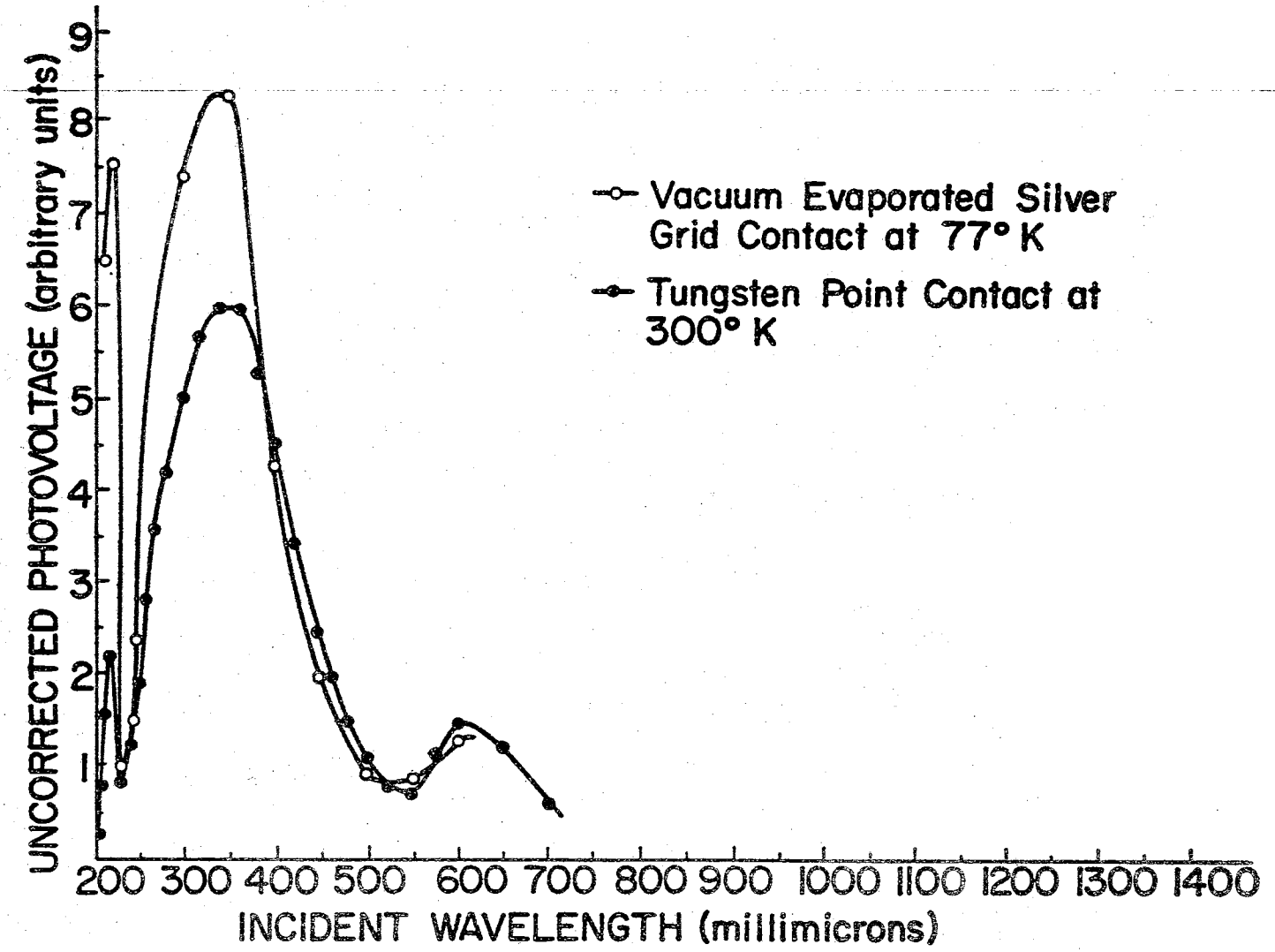

Fig. 29. Experimental photovoltage using a hydrogen lamp source.

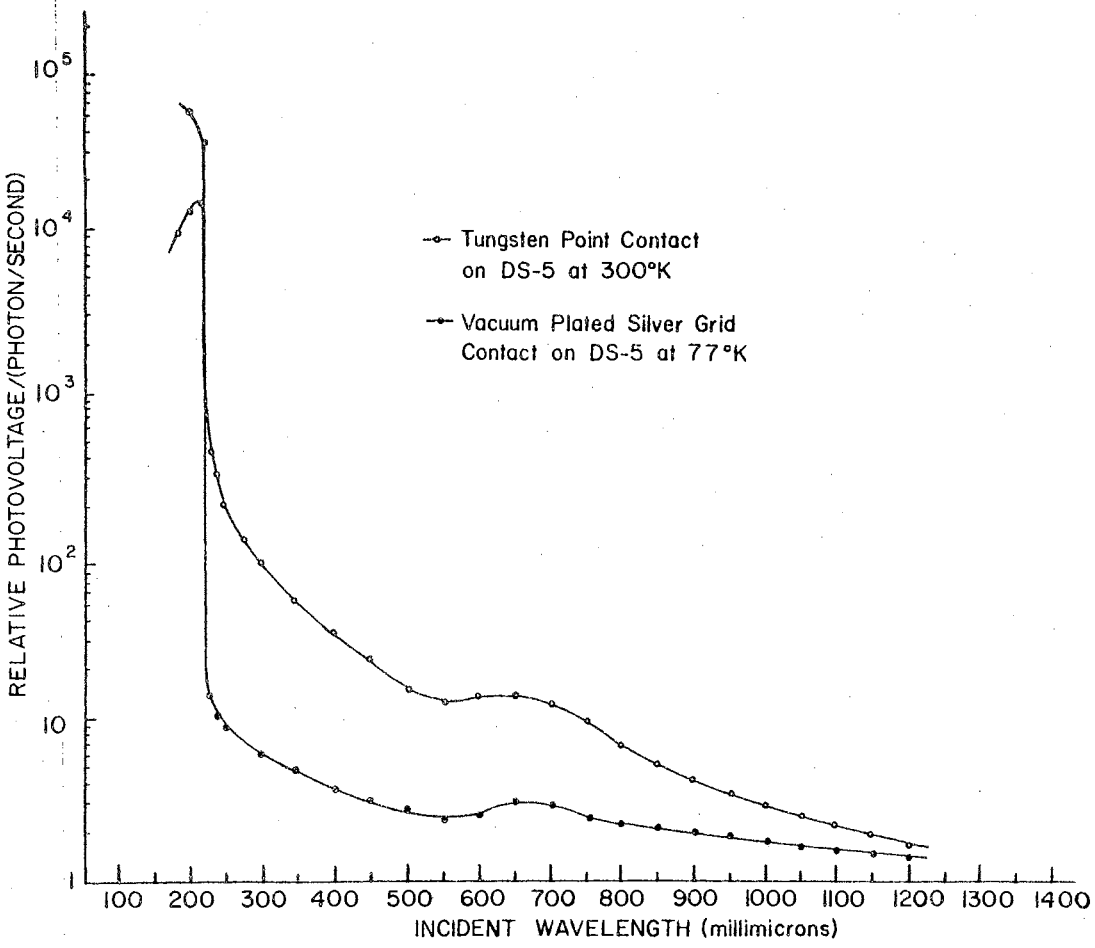

Fig. 30. Spectral response of the photovoltage at a diamond to metal contact at two temperatures.

same shift with temperature as is shown in the optical absorption. As the energy of the incident photon approaches that of the energy gap, phonons can provide the additional energy required for the electrons to jump the gap. When this occurs, an increase in the optical absorption and in the photovoltage is observed. If the temperature is lowered, the number of high energy phonons is reduced. This results in a lower optical absorption and photovoltage at that wavelength. Some of the structure observed in the photoconductivity was observed in the photovoltage, but due to lower signal to noise ratios of the photovoltage, all of the fine structure was not resolved.

The temperature dependence of the photovoltage at the diamond to metal contact is shown in Fig. 31. The dramatic increase in the photovoltage as the temperature is lowered is evident for example, by decreasing the temperature from 180°K to 130°K which increases the photovoltage by a factor of 1000. This increased sensitivity has also been reported for germanium by Becker and Fan (35). They noted that the increased sensitivity could not be fully accounted for by the decreased recombination rate produced by reducing the temperature. The difference in the slopes for the curves of different wavelength can be attributed to reduced phonon assisted transitions at lower temperatures.

The saturation of the photovoltage with increasing light from a mercury lamp is shown in Fig. 32. The limiting photovoltage is an approximation to the barrier height and was observed occasionally to be as high as 0.6 volts. The photovoltage is observed to be proportional to the light intensity at low light levels, and this

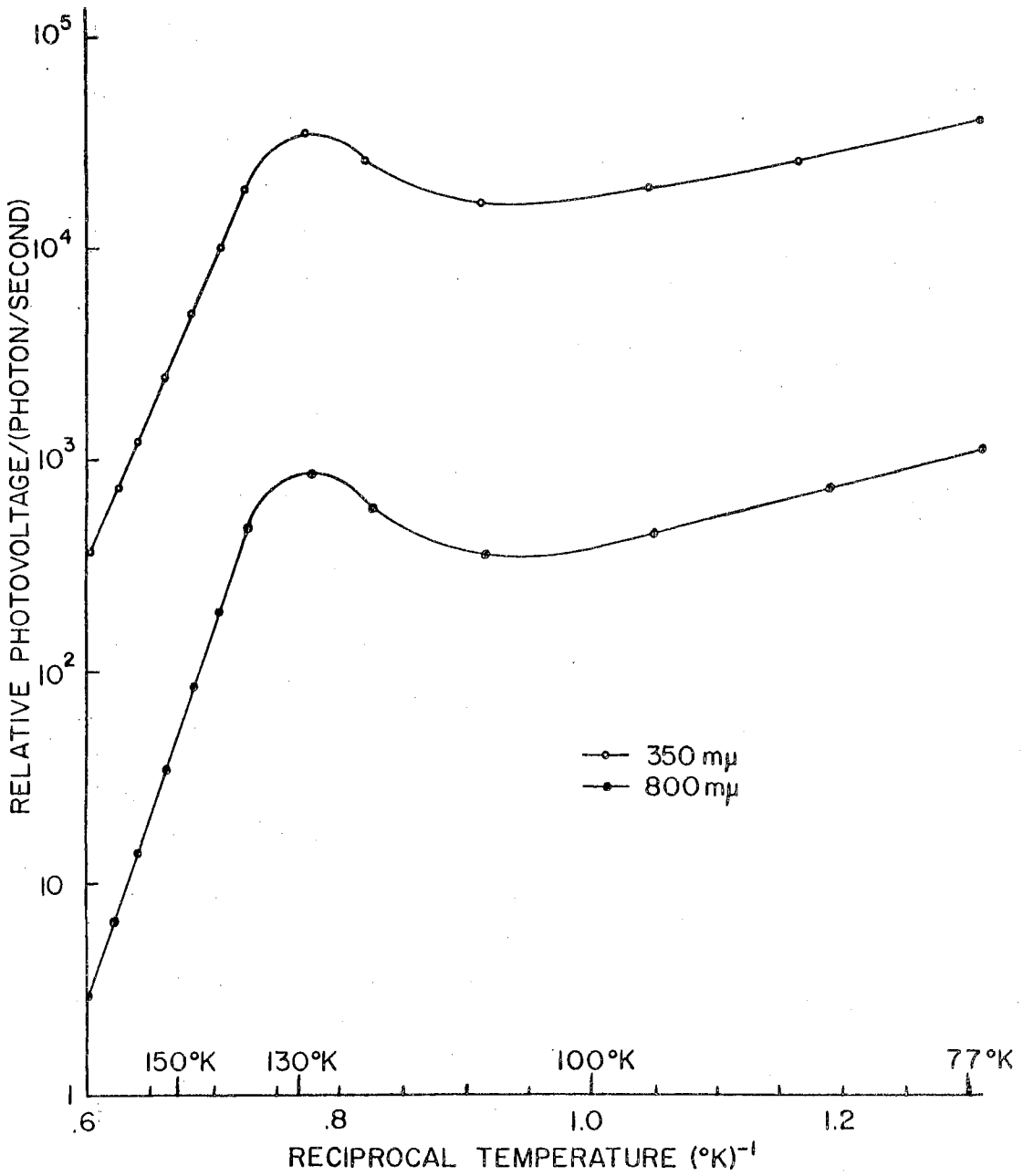

Fig. 31. The temperature dependence of the photovoltage for two wavelengths of light.

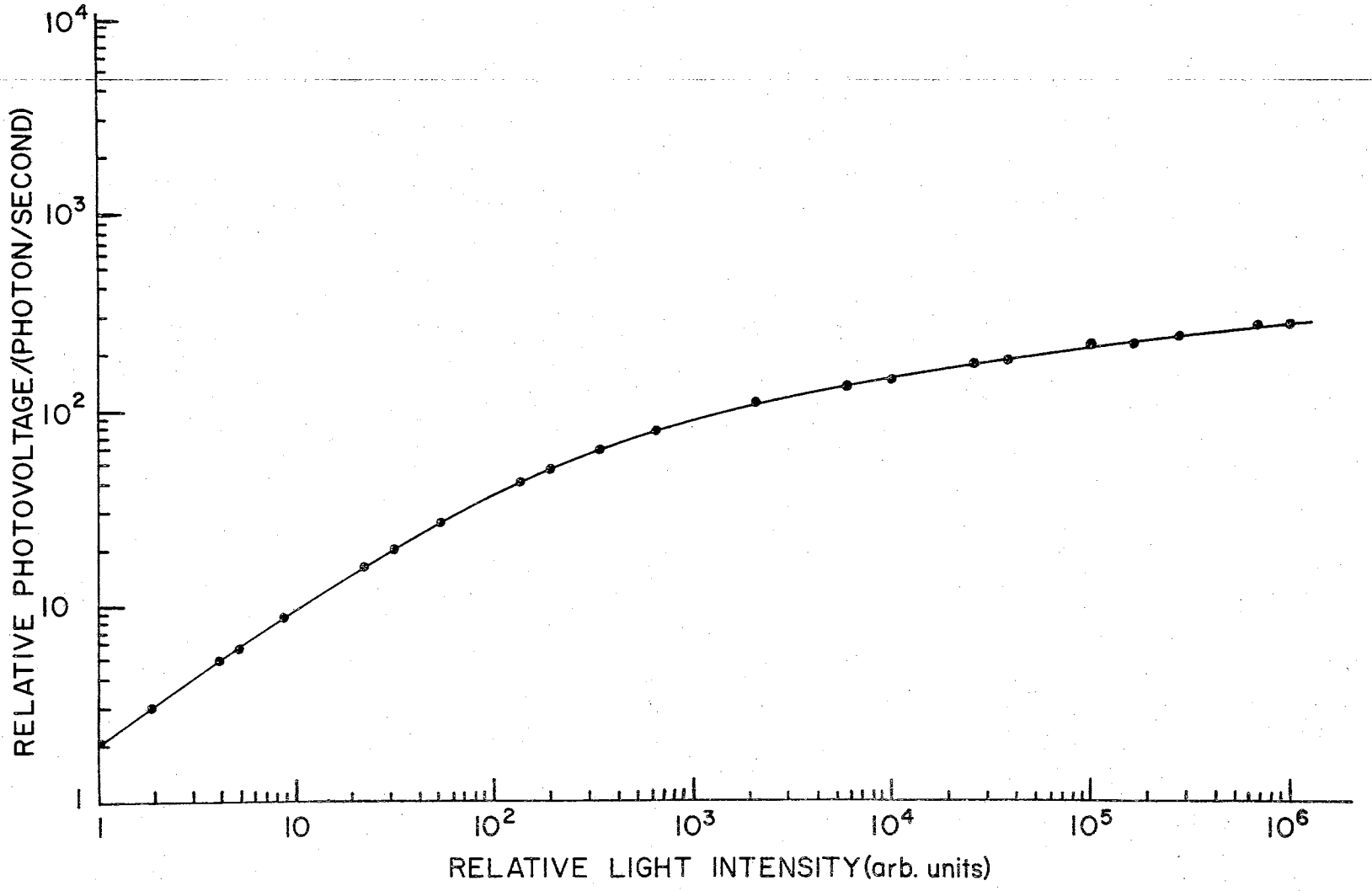

Fig. 32. The variation of the photovoltage with intensity of light.

is the intensity range used to make most of the measurements of the photovoltage.

CHAPTER IV

INTERPRETATION OF RESULTS

Summary and Conclusions

The results of this study of the photovoltage at a diamond to metal contact are summarized below.

1. A direct measurement on diamond has been made to determine some of the properties of the energy bands at the diamond surface. The conclusions drawn agree with the rectification studies by Bell (34) and indicate that the surface presents a barrier to holes moving from the semiconductor to the metal. The polarity of the illuminated contact shows that the holes move into the diamond bulk in greater numbers than electrons. That is, the diamond becomes positive with respect to the metal at the illuminated contact. The maximum photovoltage measured in the experiment of the photovoltage vs intensity of illumination was 0.6 volts. Extrapolation of the curve indicates the potential barrier may be as high as 0.8 volts. The height of the barrier is not in general constant over the surface of the diamond.

2. The correlation between the magnitude of the photovoltage as measured by the electrometer and the diamond's bulk properties

shows that diamonds with both a high bulk resistivity and high photoconductivity display a higher apparent photovoltage than diamonds with a high bulk resistivity and low photoconductivity. One explanation for this effect is found in the discussion in Chapter II concerning the effect of the bulk resistance of the sample R_s on the electrometer's output. When R_s is comparable to or greater than the input resistance of the electrometer, the high photoconductivity of a sample lowers R_s so that the electrometer reads a higher voltage than if R_s were constant.

Robertson, Fox, and Martin's (1) observation that Type II diamonds in general display a higher photovoltage than Type I diamonds is consistent with the observations of the present investigation. Thus a Type II diamond which is a poor photoconductor may still produce a photovoltage of several hundred millivolts. However the highest photovoltages are obtained with Type II diamonds which are good photoconductors or have initially low resistances.

3. No correlation was observed between the strength and the color of the luminescence, and the magnitude of the photovoltage.

4. The time dependence of the photovoltage was a primary factor which determined the manner by which many of the measurements were to be made. The existence of the time dependence precluded using a "bucking voltage" to obtain an open circuit photovoltage. Therefore, the open circuit photovoltage was approximated by using an electrometer with an input resistance of 10^{12} ohms. The electrometer used was capable of measuring 10^{-17} amps.

The time dependence of the photovoltage produced by wavelengths

greater than the energy gap indicates there is an accumulation of charge in the slow states which compensates the inner charge. The establishment of the "reverse" dipole layer is further evidenced by the reverse polarity which results when the initial light is removed corresponding to discharging of the populated slow states. The reverse polarity is very similar in strength and time dependence to the initial photovoltage. Time dependent photovoltages have been observed in germanium and are explained by the presence of slow states at the germanium surface. This model was established for the "free surface" of a semiconductor and indicates that the theory of the free surface must be included to some degree when discussing the metal contact to a diamond.

Another reverse dipole layer may exist at the nonilluminated contact. This reverse dipole can act to cancel the initial photovoltage when only one carrier is produced.

5. The behavior of the photovoltage has been classified into three types. The first type of behavior is found at room temperature at specific locations on the diamond. The polarity of the diamond with respect to the metal depends upon the location of the illuminated probe on the diamond. For this type of behavior a metal point probe can be used as the illuminated electrical contact and an evaporated metal, low melting point metal, or silver paint used as the other electrical contact. It should be noted that point probes are characterized by their applying strong local pressures, having weakly adhering bonds, and covering small surface areas. This type of behavior was not found as frequently on the Type IIb diamonds as it

was with the Type I and Type IIa. In a typical examination with the point probe, a surface area on the diamond shaped like a disc with a diameter of 1/32 of an inch produces a photovoltage up to 0.6 volts. There is frequently a central point in the disc where the signal is optimized. This suggests a local defect on or near the surface of the diamond which is not necessarily visible but which produces the potential barrier. This type of photovoltage exhibits a time decay and therefore has an associated reverse polarity dipole layer.

In the second type of photovoltage a titanium hydride contact was used as the ohmic contact to diamond and a tungsten whisker as the point probe. This type of photovoltage was observed at room temperature and did not show the time dependent decay observed in the other measurements. Instead, the photovoltage quickly reached a constant value which it maintained much as in a p-n photocell. The time dependence indicates an opposing dipole layer was not established to cancel the initial photovoltage. The source of the photovoltage is probably a local surface defect as it was found at only one small area of the diamond and is influenced by liquid metals on the surface.

The third type of behavior was observed in all Type IIb diamonds examined. The photovoltage exhibits the time dependent decay found in transient photovoltages, but the polarity was not a function of the location of the probe on the diamond surface. This type of behavior is undetectable at room temperature and first appears near 200°K. The magnitude of the photovoltage increases by a factor of one thousand between 200°K and 120°K. A saturation of the photovoltage was noted as the temperature was reduced. Interpretations of the

saturation are difficult since at these temperatures (77°K) the resistance of the bulk of the sample approached the input impedance of the electrometer. The increased fraction of the photovoltage that is dropped across the sample bulk results in an apparent reduction in the photovoltage as measured by the electrometer. The saturation observed may therefore be due to a combination of processes.

Two types of behavior of the photovoltage can therefore be associated with a surface defect. One of the types is transient due to a reverse dipole being established at the contact, and the other can produce a constant photovoltage.

When a region of a Type IIb diamond is found to produce a transient photovoltage at room temperature, the sensitive region can be vacuum plated with a metal contact, and the third type of behavior will result. No longer will a photovoltage be produced at room temperature. However surfaces which apparently do not have a region sensitive to the photovoltage may also produce the third type of behavior.

5. The spectral response of the photovoltage was measured from 2000 Angstroms to 2.0 microns. The sharp rise at 2200 Angstroms occurs when the electrons jump the energy gap by absorbing a photon's energy. The mobile electron is then able to move into the metal while the corresponding hole in the semiconductor is impeded by the potential barrier at the surface. Since optical absorption has a high probability of occurring with photons of this energy, and this absorption takes place near the surface where many electrons will diffuse across into the metal, a marked increase in the photovoltage

occurs. A much smaller increase in the photovoltage occurs near 6750 Angstroms and is probably associated with the states that give rise to the photoconductivity spectra. The states associated with the infrared wavelengths which dominate the photoconductivity response at low temperatures do not contribute appreciably to the low temperature photovoltage. The photovoltaic spectral response displayed an analogous behavior to the optical absorption near the ultraviolet absorption edge indicating that transitions are made across the gap with photon energies less than the energy of the gap. The assistance of phonons in these cases is evidenced by the difference in slopes of the temperature dependence of the photovoltaic spectrum.

Suggestions for Further Study

The production of man made diamonds will greatly assist the research on diamond. By controlled preparation, many of the complications found in natural specimens can be avoided. Energy levels are being quickly identified with specific impurities, and it may soon be possible to produce an n-type diamond. Subsequent developments will probably include ultraviolet lasers and high temperature semiconducting devices.

BIBLIOGRAPHY

1. R. Robertson, J. J. Fox, and A. E. Martin, "Two Types of Diamond," Proc. Roy. Soc. (London) 232, 463 (1934).

2. J. F. H. Custers, "Unusual Phosphorescence of a Diamond," Physica 18, 489 (1952).

3. J. F. H. Custers, "Type IIb Diamonds," Physica 20, 183 (1954).

4. W. J. Leivo and R. Smoluchowski, "A Semiconducting Diamond," Phys. Rev. 98, 1532 (1955).

5. J. J. Brophy, "Preliminary Study of the Electrical Properties of Semiconducting Diamond," Phys. Rev. 99, 1336 (1955).

6. M. D. Bell and W. J. Leivo, "Rectification, Photoconductivity and Photovoltaic Effect in Semiconducting Diamond," Phys. Rev. 111, 1227 (1958).

7. J. J. Charette, "Le Spectre Infra-Rouge A. Grande Disperson Des Trois Types De Diamants Et Ses Variations En Fonction De La Temperature," Physica 25, 1303 (1959).

8. J. J. Charette, "Essai De Classification Des Bandes D'Absorption Infra-Rouge Du Diamont, "Physica 27, 1061 (1961).

9. R. J. Collins and H. Y. Fan, "Infrared Lattice Absorption Bands in Germanium, Silicon and Diamond," Phys. Rev. 93, 674 (1954).

10. K. Lonsdale, Acta Cryst. 1, 142 (1948).

11. M. Lax and E. Burstein, "Infrared Lattice Absorption in Ionic and Homopolar Crystals," Phys. Rev. 97, 39 (1955).

12. J. L. Birman, "Theory of Infrared and Raman Processes in Crystals: Selection Rules in Diamond and Zincblende," Phys. Rev. 131, 1489 (1963).

13. C. Johnson, H. Stein, T. Young, J. Wayland and W. J. Leivo, "Photoeffects and Related Properties of Semiconducting Diamonds," J. Phys. Chem. Solids 25, 827 (1964).

14. A. Halperin and J. Nahum, "Some Optical and Electrical Properties of Semiconducting Diamonds," J. Phys. Chem. Solids 18, 297 (1961).

15. J. R. Hardy and S. D. Smith, "Two-phonon Infrared Lattice Absorption in Diamond," Phil. Mag. 6, 1163 (1961).

16. J. R. Hardy, S. D. Smith, and W. Taylor, "Optical Phonon Effects in Absorption and Photoconductivity of Semiconducting Diamond," Proceedings of the International Conference of the Physics of Semiconductors, Exeter, July, 1962.

17. J. B. Krumme, "Photoconductivity in Semiconducting Diamonds at Low Temperatures," Doctoral Thesis, Oklahoma State University, Stillwater, Oklahoma, 1965.

18. J. H. Wayland and W. J. Leivo, "Lifetimes and Trapping of Carriers in Semiconducting Diamonds," Bull. Am. Phys. Soc. 3, 400 (1958).

19. R. Wolfe and J. Woods, "Electroluminescence of Semiconducting Diamonds," Phys. Rev. 105, 921 (1957).

20. J. C. Male, "Luminescense Excitation Spectrum of Diamond Near the Fundamental Absorption Edge," Proc. Phys. Soc. 77, 869 (1961).

21. J. C. Male and J. R. Prior, "Intrinsic Recombination Radiation in Diamond," Nature 186, 1037 (1960).

22. J. B. Krumme and W. J. Leivo, "Luminescense in Semiconducting Diamond," Bull. Am. Phys. Soc. 5, 187 (1960).

23. M. D. Bell, "Electron Spin Resonance in Diamond," Doctoral Thesis, Oklahoma State University, Stillwater, Oklahoma, 1964.

24. W. Kaiser and W. L. Bond, "Nitrogen, A Major Impurity in Common Type I Diamond," Phys. Rev. 115, 857 (1959).

25. C. J. Rauch, "Millimeter Cyclotron Resonance in Diamond," Proceedings of the International Conference of the Physics of Semiconductors, Exeter, July, 1962.

26. R. Mykolajewycz, J. Kalnajs, and A. Smakula, "High-Precision Density Determination of Natural Diamonds," J. Appl. Phys. 35, 1773 (1964).

27. C. Kittel, Introduction to Solid State Physics (John Wiley and Sons, Inc., New York, 1957) 2nd ed.

28. W. Shockley, Electrons and Holes in Semiconductors (D. Van Nostrand Co., Inc., New York, 1956).

29. J. Tauc, Photo and Thermoelectric Effects in Semiconductors (Pergamon Press, New York, 1962).

30. W. Schottky, Zeits. F. Physik 118, 539 (1942).

31. L. P. Hunter, Handbook of Semiconductor Electronics (McGraw-Hill Book Company, Inc., New York, 1956).

32. E. O. Johnson, "Comparison of the Semiconductor Surface and Junction Photovoltages," RCA Rev. 18, 556 (1957).

33. J. Bardeen, "Surface States and Rectification at a Metal Semiconductor Contact," Phys. Rev. 71, 717 (1947).

34. D. Pugh, "Surface States on the (111) Surface of Diamond," Phys. Rev. Letters 12, 390 (1964).

35. M. D. Bell, "Rectification and Photoeffects in Semiconducting Diamonds," Masters Thesis, Oklahoma State University, Stillwater, Oklahoma, 1956.

36. M. Becker and H. Y. Fan, "Photovoltaic Effect of P-N Junctions in Germanium," Phys. Rev. 78, 301 (1950).

VITA

Clyde John Marshall Northrup, Jr.

Candidate for the Degree of

Doctor of Philosophy

Thesis: PHOTOVOLTAGE AT AT A METAL TO DIAMOND CONTACT

Major Field: Physics

Biographical:

Personal Data: Born in Oklahoma City, Oklahoma, April 25, 1938, the son of Clyde J.M. and Gladys Northrup, Sr.

Education: Attended grade school in Oklahoma City, Oklahoma, Honolulu, Hawaii, and Albuquerque, New Mexico in 1956; received a Bachelor of Science degree in Mathematics in January 1961 and a Bachelor of Science degree in Physics in May 1961 from Oklahoma State University; completed requirements for the Doctor of Philosophy degree in May, 1966.

Professional experience: Employed by Sandia Corporation, in Albuquerque, New Mexico during the summers of 1958, 1959, and 1960. Commissioned into the United States Army in July 1961 and is presently a First Lieutenant assigned to the U.S. Army Foreign Science and Technology Center in Washington, D.C.

Organizations: Member of American Association of Physics Teachers, Sigma Pi Sigma, and Omicron Delta Kappa.